Dalton
www.rsc.org/dalton

The substitution chemistry of the tris(3,5-dimethylpyrazolyl)-methanerhodium complex $[Rh(CO)_2\{HC(pz')_3\}]^+$

Christopher J. Adams,[a] **Neil G. Connelly,***[a] **David J. H. Emslie,**[a] **Owen D. Hayward,**[a] **Tania Manson,**[a] **A. Guy Orpen**[a] **and Philip H. Rieger**[b]
[a] *School of Chemistry, University of Bristol, Bristol, UK BS8 1TS*
[b] *Department of Chemistry, Brown University, Rhode Island, RI 02912, USA*

Received 3rd March 2003, Accepted 23rd May 2003
First published as an Advance Article on the web 20th June 2003

The complex $[Rh(CO)_2\{HC(pz')_3\}][PF_6]$, $\mathbf{1}^+[PF_6]^-$ $\{HC(pz')_3$ = tris(3,5-dimethylpyrazolyl)methane$\}$, prepared by reacting $[\{Rh(CO)_2(\mu\text{-}Cl)\}_2]$ with $HC(pz')_3$ in the presence of $Tl[PF_6]$, has a distorted square pyramidal structure with a κ^3-$HC(pz')_3$ ligand. Carbonyl substitution with Lewis bases gives $[Rh(CO)L\{HC(pz')_3\}][PF_6]$ $\{L = PPh_3$, $\mathbf{2}^+[PF_6]^-$; $L = AsPh_3$, $\mathbf{3}^+[PF_6]^-$; $L = P(o\text{-tolyl})_3$, $\mathbf{4}^+[PF_6]^-\}$, which have square planar κ^2 structures, confirmed by X-ray crystallography for $\mathbf{2}^+[PF_6]^-$. The cations $\mathbf{2}^+$ and $\mathbf{3}^+$ have the third pyrazolyl ring orientated *pseudo*-parallel to the square planar metal whereas $\mathbf{4}^+$ more likely has the third ring orientated *exo* to that plane. One-electron oxidation of $\mathbf{2}^+$ and $\mathbf{3}^+$ gives the Rh(II) dications $[Rh(CO)(PPh_3)\{HC(pz')_3\}]^{2+}$, $\mathbf{2}^{2+}$, and $[Rh(CO)(AsPh_3)\{HC(pz')_3\}]^{2+}$, $\mathbf{3}^{2+}$, characterised by ESR spectroscopy. Complex $\mathbf{1}^+[PF_6]^-$ reacts with PhC≡CPh to give $[Rh(CO)(\eta^2\text{-}PhC{\equiv}CPh)\{HC(pz')_3\}][PF_6]$, $\mathbf{5}^+[PF_6]^-$, in which the two-electron donor alkyne occupies an equatorial position in a trigonal bipyramidal κ^3 structure. With MeC≡CR (R = Me or Et), $\mathbf{1}^+[PF_6]^-$ gives the κ^2 square planar complexes $[Rh\{\eta^4\text{-}C_4Me_2R_2C(O)\}\{HC(pz')_3\}][PF_6]$ (R = Me, $\mathbf{6}^+[PF_6]^-$; R = Et, $\mathbf{7}^+[PF_6]^-$) in which the cyclopentadienone ligands are coordinated *via* two Rh–monoalkene bonds; the structurally characterised form of $\mathbf{7}^+$ has the two alkyne units linked head-to-head with the CEt termini bound to the ketonic CO group. With HC≡CPh or HC≡CH, $\mathbf{1}^+$ gives the octahedral, κ^3 rhodium(III) metallacyclopentadienes $[Rh(CO)(\eta^1{:}\eta^{1'}\text{-}CHCRCHCR)\{HC(pz')_3\}][PF_6]$ (R = Ph, $\mathbf{8}^+[PF_6]^-$; R = H, $\mathbf{9}^+[PF_6]^-$) with the two alkynes linked head-to-tail in $\mathbf{8}^+$. The reaction of $\mathbf{1}^+$ with HC≡CH also gives the cycloheptatrienone (tropone) derivative $[Rh\{\eta^4\text{-}C_6H_6C(O)\}\{HC(pz')_3\}][PF_6]$, $\mathbf{10}^+[PF_6]^-$, with a κ^3 ligand and the cycloheptatrienone ligand bound to the metal *via* two Rh–C σ-bonds and one Rh–monoalkene interaction.

Introduction

Tris(3,5-dimethylpyrazolyl)methane, $HC(pz')_3$, is a neutral analogue of the hydrotris(3,5-dimethylpyrazolyl)borate anion, $[HB(pz')_3]^-$ (Tp'^-), and may also be considered related to arenes, C_6R_6, in that both are neutral six-electron donors (*cf.* the formal relationship between Tp'^- and the cyclopentadienide anions $C_5R_5^-$). Rhodium complexes of hydrotris(pyrazolyl)borate anions are well studied,[1–8] particularly dicarbonyls such as $[Rh(CO)_2Tp']$ which act as photocatalysts for the activation of hydrocarbons.[9] By contrast, there are relatively few rhodium complexes of tris(pyrazolyl)methane ligands, *e.g.* $[RhL_2\{HC(pz)_3\}][RhCl_2L_2]$ $\{pz$ = pyrazolyl, L_2 = cycloocta-1,5-diene (cod), norbornadiene (nbd), tetrafluorobenzobarrelene (tfb) or $(CO)_2\}$, $[Rh(cod)\{HC(pz)_3\}][ClO_4]$ and $[Rh(nbd)\{HC(pz)_3\}][PF_6]$.[10,11]

Our discovery[12] that one-electron oxidation of $[Rh(CO)LTp']$ $\{L = PPh_3, P(NMe_2)_3$, *etc.*$\}$ gave stable Rh(II) cations $[Rh(CO)LTp']^+$ led us to investigate the possibility of similar behaviour for tris(3,5-dimethylpyrazolyl)methane analogues. We now describe the synthesis of $[Rh(CO)_2\{HC(pz')_3\}][PF_6]$ $\mathbf{1}^+[PF_6]^-$, its reactions with Lewis bases, L, to give redox-active $[Rh(CO)L\{HC(pz')_3\}][PF_6]$, and the isolation of a variety of organometallic products with alkynes which differ from those formed with the cyclopentadienyl analogues $[Rh(CO)_2(\eta\text{-}C_5R_5)]$ (R = H, Me, *etc.*).[13–18]

Results and discussion

Synthesis and characterisation of $[Rh(CO)_2\{HC(pz')_3\}][PF_6]$, $\mathbf{1}^+[PF_6]^-$

The reaction of $[\{Rh(CO)_2(\mu\text{-}Cl)\}_2]$ with two equivalents of $HC(pz')_3$ in CH_2Cl_2 gave a solution of $[Rh(CO)_2\{HC(pz')_3\}][Rh(CO)_2Cl_2]$[11] {and unreacted $HC(pz')_3$} to which two equivalents of $Tl[PF_6]$ were added to give yellow crystals of $[Rh(CO)_2\{HC(pz')_3\}][PF_6]$, $\mathbf{1}^+[PF_6]^-$, characterised by elemental analysis, IR (Table 1) and NMR spectroscopy (Table 2) and X-ray crystallography.

The IR spectrum of $\mathbf{1}^+[PF_6]^-$ in CH_2Cl_2 shows four carbonyl bands, at 2099w, 2079s, 2039w and 2011s cm^{-1}. For analogous rhodium dicarbonyl hydrotris(pyrazolyl)borate complexes three isomers have been identified (Fig. 1); ν(CO) is higher in energy for the κ^2 forms (A and B) than the κ^3 form (C).[4–7] Which of the three isomers is observed depends on the pyrazolyl ring substituents (and, when CO substitution occurs, on the ligand, L, of $[Rh(CO)LTp']$ [12]). Thus, the IR spectrum of $\mathbf{1}^+$ suggests two isomers in solution, in an approximate 1 : 10 ratio, *i.e.* with κ^2 (2099 and 2039 cm^{-1}) and κ^3 structures (2079 and 2011 cm^{-1}) respectively. By contrast, the Nujol IR spectrum (Table 1) suggests $\mathbf{1}^+[PF_6]^-$ exists only as the κ^3 isomer in the solid state, confirmed by X-ray crystallography (see below), and as suggested for the hydrotris(3,5-dimethylpyrazolyl)borate complex $[Rh(CO)_2Tp']$.[4] (The analogue $[Rh(CO)_2L]$ $\{L$ = hydrotris(3-trifluoromethyl-5-methylpyrazolyl)borate$\}$ does adopt[7] the κ^3 form in the solid state, though the sterically crowded compound $[Rh(CO)_2L]$ $\{L$ = hydrotris(3-phenyl-5-methylpyrazolyl)borate$\}$ has a κ^2 structure.[8])

The X-ray structure of $\mathbf{1}^+[PF_6]^-$ (Fig. 2; selected bond lengths and angles in Table 3) confirms the $HC(pz')_3$ ligand to be κ^3

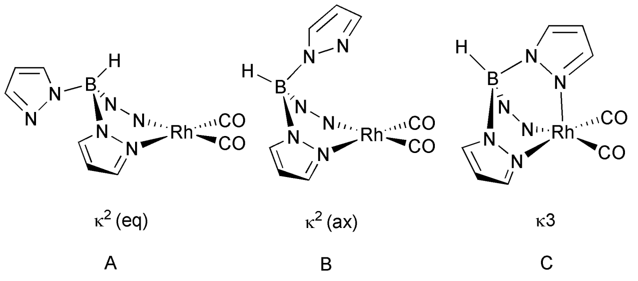

Fig. 1 The isomers of $[Rh(CO)_2Tp]$.

DOI: 10.1039/b302440g

Table 1 Analytical data for rhodium tris(3,5-dimethylpyrazolyl)methane complexes

Complex	Colour	Yield (%)	Analysis (%)[a] C	H	N	IR/cm^{-1}[b] ν(CO)
$[Rh(CO)_2\{HC(pz')_3\}][PF_6]$, $\mathbf{1}^+[PF_6]^-$	Yellow	94	35.7 (35.9)	3.4 (3.7)	13.6 (14.0)	2099w, 2039w;[c] 2079, 2011;[d] 2083, 2074, 2014, 2004[e]
$[Rh(CO)(PPh_3)\{HC(pz')_3\}][PF_6]{\cdot}CH_2Cl_2$, $\mathbf{2}^+[PF_6]^-{\cdot}CH_2Cl_2$	Yellow	64	47.0 (46.9)	4.1 (4.3)	9.0 (9.1)	2000
$[Rh(CO)(AsPh_3)\{HC(pz')_3\}][PF_6]{\cdot}CH_2Cl_2$, $\mathbf{3}^+[PF_6]^-{\cdot}CH_2Cl_2$	Yellow	72	44.5 (44.8)	3.7 (4.1)	8.4 (8.7)	1996
$[Rh(CO)\{P(o\text{-tolyl})_3\}\{HC(pz')_3\}][PF_6]{\cdot}0.5CH_2Cl_2$, $\mathbf{4}^+[PF_6]^-{\cdot}0.5CH_2Cl_2$	Yellow	29	50.0 (50.2)	4.8 (4.8)	8.9 (9.1)	1977
$[Rh(CO)(\eta^2\text{-PhC}{\equiv}CPh)\{HC(pz')_3\}][PF_6]{\cdot}CH_2Cl_2$, $\mathbf{5}^+[PF_6]^-{\cdot}CH_2Cl_2$	Fawn	54	45.7 (45.9)	4.2 (4.1)	11.0 (10.0)	2043
$[Rh\{\eta^4\text{-}C_4Me_4C(O)\}\{HC(pz')_3\}][PF_6]$, $\mathbf{6}^+[PF_6]^-$	Dark red	59	43.8 (43.0)	4.7 (5.0)	11.9 (12.3)	1667
$[Rh\{\eta^4\text{-}C_4Me_2Et_2C(O)\}\{HC(pz')_3\}][PF_6]{\cdot}0.5CH_2Cl_2$, $\mathbf{7}^+[PF_6]^-{\cdot}0.5CH_2Cl_2$	Dark red	65	43.7 (43.9)	5.6 (5.2)	11.4 (11.2)	1661
$[Rh(CO)(\eta^1{:}\eta^{1'}\text{-CHCPhCHCPh})\{HC(pz')_3\}][PF_6]$, $\mathbf{8}^+[PF_6]^-$	Cream	90	50.7 (50.9)	3.6 (4.4)	10.1 (10.7)	2083
$[Rh(CO)(\eta^1{:}\eta^{1'}\text{-}C_4H_4)\{HC(pz')_3\}][PF_6]$, $\mathbf{9}^+[PF_6]^-$	Pale yellow	42	40.1 (40.3)	3.8 (4.2)	13.3 (13.4)	2080

[a] Calculated values in parentheses. [b] In CH_2Cl_2 unless stated otherwise. [c] κ^2-isomer. [d] κ^3-isomer. [e] In Nujol.

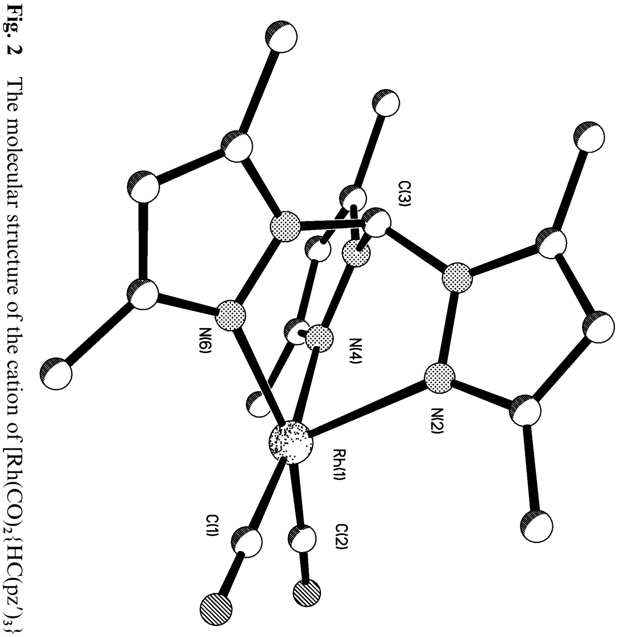

Fig. 2 The molecular structure of the cation of $[Rh(CO)_2\{HC(pz')_3\}][PF_6]$, $\mathbf{1}^+[PF_6]^-$. Hydrogen atoms have been omitted for clarity.

co-ordinated with the rhodium atom in a distorted square pyramid. The axial Rh(1)–N(2) bond (average value of 2.44 Å for the two independent molecules in the unit cell) is longer than the Rh(1)–N(4) and Rh(1)–N(6) bonds in the square plane (average value 2.13 Å). The angles N(6)–Rh(1)–C(2) and N(4)–Rh(1)–C(1) across this plane are less than 180° (average values 163.4 and 173.7°, respectively), and thus the molecule has adopted an elevated square pyramidal geometry, raising the rhodium atom above the square plane towards the apical nitrogen atom. It therefore lies on the reaction coordinate for the formation of trigonal bipyramidal complexes from square pyramidal intermediates.[19] This may be compared with the flattened square pyramidal geometry adopted by $[Rh(CO)\{P(OPh)_3\}Tp']$, with a longer apical rhodium–nitrogen distance of 2.764(2) Å, and angles across the basal plane of 176.0(1) and 178.0(1)°.[12]

Reactions of $[Rh(CO)_2\{HC(pz')_3\}][PF_6]$, $\mathbf{1}^+[PF_6]^-$

Cationic $[Rh(CO)_2\{HC(pz')_3\}]^+$, $\mathbf{1}^+$, appears to be more reactive towards Lewis bases than is the neutral analogue $[Rh(CO)_2Tp']$.[12] For example, the reaction of the latter with PPh_3 in *n*-hexane under reflux was complete only after 24 hours, whereas that between $\mathbf{1}^+$ and PPh_3 in CH_2Cl_2, to give $[Rh(CO)(PPh_3)\{HC(pz')_3\}][PF_6]$, $\mathbf{2}^+[PF_6]^-$, was complete in five minutes. In addition, $[Rh(CO)_2Tp']$ did not react with $AsPh_3$ or $P(o\text{-tolyl})_3$ whereas $\mathbf{1}^+$ and $AsPh_3$ in CH_2Cl_2 gave a yellow solution of $[Rh(CO)(AsPh_3)\{HC(pz')_3\}][PF_6]$, $\mathbf{3}^+[PF_6]^-$, after four days, and heating a thf solution of $\mathbf{1}^+[PF_6]^-$ with $P(o\text{-tolyl})_3$ under reflux for two days gave $[Rh(CO)\{P(o\text{-tolyl})_3\}\{HC(pz')_3\}][PF_6]$, $\mathbf{4}^+[PF_6]^-$. The reaction of $\mathbf{1}^+$ with $P(OPh)_3$ in CH_2Cl_2 for four hours gave a yellow solution showing ν(CO) at 2030 cm^{-1}, consistent with the formation of $[Rh(CO)\{P(OPh)_3\}\{HC(pz')_3\}]^+$, but the product could not be isolated.

With halides, $HC(pz')_3$ displacement occurs from $\mathbf{1}^+$, giving the anions $[RhX_2(CO)_2]^-$ (X = Cl, Br, I).[20] The reactions with Lewis bases show, therefore, that although the additional positive charge of $\mathbf{1}^+$ (*cf.* neutral $[Rh(CO)_2Tp']$) weakens the Rh–CO bonds, leading to carbonyl substitution products more readily, $HC(pz')_3$ is also more easily displaced, *cf.* the hydrotris(3,5-dimethylpyrazolyl)borate anion.

Characterisation of $[Rh(CO)L\{HC(pz')_3\}][PF_6]$, $\mathbf{2}^+[PF_6]^-$–$\mathbf{4}^+[PF_6]^-$

Complexes $\mathbf{2}^+[PF_6]^-$–$\mathbf{4}^+[PF_6]^-$ were characterised by elemental analysis and IR (Table 1) and ^1H, ^{13}C–$\{^1H\}$ and ^{31}P NMR

Table 2 Proton, ^{13}C–{^{1}H} and ^{31}P NMR spectroscopic data for rhodium tris(3,5-dimethylpyrazolyl)methane complexes[a]

Complex	^{1}H	^{13}C–{^{1}H}	^{31}P
[Rh(CO)$_2${HC(pz′)$_3$}][PF$_6$], **1**$^+$[PF$_6$]$^-$	7.84 {s, 1H, *H*C(pz′)$_3$}, 6.17 (s, 3H, pz′ CH), 2.54 (d, 9H, *J* 1, pz′ CH$_3$), 2.46 (s, 9H, pz′ CH$_3$)	185.83 (d, $J_{\mathrm{C,Rh}}$ 71, CO), 154.48 (d, *J* 1, pz′ *C*CH$_3$), 142.93 (s, pz′ *C*CH$_3$), 109.07 (s, pz′ CH), 69.71 {s, H*C*(pz′)$_3$}, 15.42 (s, pz′ CH$_3$), 11.29 (s, pz′ CH$_3$)	—
[Rh(CO)(PPh$_3$){HC(pz′)$_3$}][PF$_6$], **2**$^+$[PF$_6$]$^-$	7.68 {s, 1H, *H*C(pz′)$_3$}, 7.50–7.35 (m, 15H, PPh$_3$), 5.99 (s, 3H, pz′ CH), 2.26 (s, 9H, pz′ CH$_3$), 1.84 (s, 9H, pz′ CH$_3$)	188.13 (dd, $J_{\mathrm{C,Rh}}$ 73, $J_{\mathrm{C,P}}$ 24, CO), 154.27 (s, pz′*C*CH$_3$), 144.04 (s, pz′*C*CH$_3$), 135–129 {m, P(C$_6$H$_5$)$_3$}, 110.06 (s, pz′CH), 75.04 {s, H*C*(pz′)$_3$}, 14.81 (s, pz′CH$_3$), 11.52 (s, pz′CH$_3$)	42.10 (d, $J_{\mathrm{P,Rh}}$ 162, PPh$_3$}, −144.45 {sept, $J_{\mathrm{P,F}}$ 710, PF$_6$)
[Rh(CO)(AsPh$_3$){HC(pz′)$_3$}][PF$_6$], **3**$^+$[PF$_6$]$^-$	7.76 {s, 1H, *H*C(pz′)$_3$}, 7.50–7.35 (m, 15H, AsPh$_3$), 5.99 (s, 3H, pz′ CH), 2.27 (s, 9H, pz′ CH$_3$), 1.86 (s, 9H, pz′ CH$_3$)	187.34 (d, $J_{\mathrm{C,Rh}}$ 70, CO), 154.19 (s, pz′ *C*CH$_3$), 144.04 (s, pz′ *C*CH$_3$), 133.6–129.5 {m, As(C$_6$H$_5$)$_3$}, 109.89 (s, pz′ CH), 75.00 {s, H*C*(pz′)$_3$}, 14.96 (s, pz′ CH$_3$), 11.50 (s, pz′ CH$_3$)	—
[Rh(CO){P(*o*-tolyl)$_3$}{HC(pz′)$_3$}][PF$_6$], **4**$^+$[PF$_6$]$^-$	8.00–6.85 {m, 12H, P(C$_6$*H*$_4$CH$_3$)$_3$}, 7.57 {s, 1H, *H*C(pz′)$_3$}, 6.36 (s, 1H, pz′ CH), 6.28 (s, 1H, pz′ C*H*), 5.89 (s, 1H, pz′ CH), 3.64 {s, 3H, pz′ CH$_3$ or P(C$_6$H$_4$C*H*$_3$)$_3$}, 2.46 {s, 6H, pz′ CH$_3$ or P(C$_6$H$_4$C*H*$_3$)$_3$}, 2.43, 1.85, 1.80, 1.49, 1.38, 1.21 {s, 3H, pz′ CH$_3$ or P(C$_6$H$_4$C*H*$_3$)$_3$}.[b]	155.76 (s, pz′ *C*CH$_3$), 154.65 (s, pz′ *C*CH$_3$), 151.78 (s, pz′ *C*CH$_3$), 145.8–140.6 {m, 3 pz′ *C*CH$_3$ and P(*C*$_6$H$_4$CH$_3$)$_3$}, 133.0–126.1 {m, P(*C*$_6$H$_4$CH$_3$)$_3$}, 111.74 (pz′ CH), 109.54 (pz′ CH), 108.63 (pz′ CH), 74.93 {H*C*(pz′)$_3$}, 25.96 {P(C$_6$H$_4$*C*H$_3$)$_3$}, 23.27 {P(C$_6$H$_4$*C*H$_3$)$_3$}, 21.83 {P(C$_6$H$_4$*C*H$_3$)$_3$}, 16.1 (pz′ CH$_3$), 13.8 (pz′ CH$_3$), 13.4 (pz′ CH$_3$), 12.1 (pz′ CH$_3$), 11.0 (pz′ CH$_3$)	30.44 {d, $J_{\mathrm{P,Rh}}$ 159, P(*o*-tolyl)$_3$}, −144.48 (sept, $J_{\mathrm{P,F}}$ 711, PF$_6$)
[Rh(CO)(η^2-PhC≡CPh){HC(pz′)$_3$}][PF$_6$], **5**$^+$[PF$_6$]$^-$	7.89 {s, 1H, *H*C(pz′)$_3$}, 7.89–7.82 (m, 4H, C$_6$H$_5$), 7.47–7.38 (m, 6H, C$_6$H$_5$), 6.28 (s, 2H, pz′ CH), 5.79 (s, 1H, pz′ CH), 2.64 (s, 6H, pz′ CH$_3$), 2.55 (s, 3H, pz′ CH$_3$), 2.51 (s, 6H, pz′ CH$_3$), 1.73 (s, 3H, pz′ CH$_3$)	184.53 (d, $J_{\mathrm{C,Rh}}$ 68, CO), 156.90 (s, pz′ *C*CH$_3$), 154.59 (s, pz′ *C*CH$_3$), 142.09 (s, pz′ *C*CH$_3$), 141.96 (s, pz′ *C*CH$_3$), 131.00, 129.70, 129.12, 128.70 (s, C$_6$H$_5$), 110.55 (s, pz′ CH), 108.82 (s, pz′ CH), 82.50 (d, $J_{\mathrm{C,Rh}}$ 16, *C*Ph), 68.45 {s, H*C*(pz′)$_3$}, 15.29 (s, pz′ CH$_3$), 13.58 (s, pz′ CH$_3$), 11.50 (s, pz′ CH$_3$), 11.08 (s, pz′ CH$_3$)	—
[Rh(CO)(η^2-PhC≡CPh){HC(pz′)$_3$}][PF$_6$], **5**$^+$[PF$_6$]$^-$ [c]	7.81 {s, 1H, *H*C(pz′)$_3$}, 7.45–7.15 (m, 10H, C$_6$H$_5$), 6.18 (s, 1H, pz′ CH), 6.11 (s, 1H, pz′ CH), 6.02 (s, 1H, pz′ CH), 2.60 (s, 3H, pz′ CH$_3$), 2.58 (s, 3H, pz′ CH$_3$), 2.54 (s, 3H, pz′ CH$_3$), 2.52 (s, 3H, pz′ CH$_3$), 2.24 (s, 3H, pz′ CH$_3$), 1.49 (s, 3H, pz′ CH$_3$)	191.28 (s, CO), 166.36 (d, $J_{\mathrm{C,Rh}}$ 22), 157.16 (d, $J_{\mathrm{C,Rh}}$ 3), 155.12 (d, $J_{\mathrm{C,Rh}}$ 6), 154.93 (s, pz′ *C*CH$_3$), 154.03 (s, pz′ *C*CH$_3$), 144.70 (s, pz′ *C*CH$_3$), 143.39 (s, pz′ *C*CH$_3$), 142.74 (s, pz′ *C*CH$_3$), 142.08 (s, pz′ *C*CH$_3$), 131.43 (s), 129.41, 129.21, 128.76, 128.71, 128.17, 127.37, 126.65, 126.38 (s, C$_6$H$_5$), 110.44 (s, pz′ CH), 108.61 (s, pz′ CH), 108.44 (s, pz′ CH), 68.93 (s, *C*Ph), 54.81 {s, H*C*(pz′)$_3$}, 15.43 (s, pz′ CH$_3$), 13.29 (s, pz′ CH$_3$), 11.79 (s, pz′ CH$_3$), 11.69 (s, pz′ CH$_3$), 10.82 (s, pz′ CH$_3$), 10.66 (s, pz′ CH$_3$)	—
[Rh{η^4-C$_4$Me$_4$C(O)}{HC(pz′)$_3$}][PF$_6$], **6**$^+$[PF$_6$]$^-$	7.37 {s, 1H, *H*C(pz′)$_3$}, 6.23 (s, 3H, pz′ CH), 2.41 (s, 9H, pz′ CH$_3$), 2.17 (s, 9H, pz′ CH$_3$), 1.92 (s, 6H, CCH$_3$), 1.06 (s, 6H, CCH$_3$)	161.73 {s, C$_4$Me$_4$*C*(O)}, 155.35 (s, pz′ *C*CH$_3$), 143.84 (s, pz′ *C*CH$_3$), 111.44 (s, pz′ CH), 95.89 (d, $J_{\mathrm{C,Rh}}$ 12, *C*$_4$Me$_4$CO), 73.90 {s, H*C*(pz′)$_3$}, 72.31 (d, $J_{\mathrm{C,Rh}}$ 9, *C*$_4$Me$_4$CO), 15.28 (s, pz′ CH$_3$), 13.01 (s, C$_4$*Me*$_4$CO), 11.46 (s, pz′ CH$_3$), 8.64 (s, C$_4$*Me*$_4$CO)	—
[Rh(CO)(η^1:η$^{1'}$-CHCPhCHCPh){HC(pz′)$_3$}][PF$_6$], **8**$^+$[PF$_6$]$^-$	7.96 {s, 1H, *H*C(pz′)$_3$}, 7.85 (dd, 1H, *J* 3, 1, H^1), 7.58–6.55 (m, 2H, Ph), 7.40–7.10 (m, 6H, Ph), 6.91–6.87 (m, 3H, H^3 and Ph), 6.23 (s, 1H, pz′ CH), 6.12 (s, 1H, pz′ CH), 5.97 (s, 1H, pz′ CH), 2.70 (s, 3H, pz′ CH$_3$), 2.63 (s, 6H, pz′ CH$_3$), 2.53 (s, 3H, pz′ CH$_3$), 2.40 (s, 3H, pz′ CH$_3$), 1.38 (s, 3H, pz′ CH$_3$)[c]	184.26 (d, $J_{\mathrm{C,Rh}}$ 71, CO), 159.56 (d, *J* 2), 159.04 (s), 155.94 (d, *J* 4), 155.57 (s), 155.13 (s), 145.97 (s)[d], 143.96 (d, $J_{\mathrm{C,Rh}}$ 2, C^3), 142.97 (s), 142.44 (d, *J* 6)[d], 139.78 (d, $J_{\mathrm{C,Rh}}$ 26, C^1), 138.18 (d, *J* 2)[d], 128.99, 128.74, 127.52, 127.30, 126.84, 125.40 (s, C$_6$H$_5$), 110.70 (s, pz′ CH), 109.38 (s, pz′ CH), 109.23 (s, pz′ CH), 68.78 {s, H*C*(pz′)$_3$}, 14.54 (s, pz′ CH$_3$), 12.99 (s, pz′ CH$_3$) 12.68 (s, pz′ CH$_3$), 11.63 (s, pz′ CH$_3$), 11.26 (s, pz′ CH$_3$), 11.15 (s, pz′ CH$_3$)	—
[Rh(CO)(η^1:η$^{1'}$-C$_4$H$_4$) {HC(pz′)$_3$}][PF$_6$], **9**$^+$[PF$_6$]$^-$	7.85 {s, 1H, *H*C(pz′)$_3$}, 7.52 (ddd, 2H *J* 5, 4, 1, H^{1,4}), 6.51 (ddd, 2H, *J* 5, 4, 2, H^{2,3}), 6.20 (s, 2H, pz′ CH), 6.00 (s, 1H, pz′ CH), 2.61 (s, 6H, pz′ CH$_3$), 2.56 (s, 3H, pz′ CH$_3$), 2.45 (s, 9H, pz′ CH$_3$)[c]	184.46 (d, $J_{\mathrm{C,Rh}}$ 71, CO), 159.02 (s, pz′ *C*CH$_3$), 155.18 (s, pz′ *C*CH$_3$), 147.65 (d, $J_{\mathrm{C,Rh}}$ 2, C^{2,3}), 145.47 (d, $J_{\mathrm{C,Rh}}$ 26, C^{1,4}), 142.39 (s, pz′ *C*CH$_3$), 142.28 (s, pz′ *C*CH$_3$), 110.32 (d, *J* 1, pz′ CH), 109.20 (s, pz′ CH), 68.67 {s, H*C*(pz′)$_3$}, 14.35 (s, pz′ CH$_3$), 12.49 (s, pz′ CH$_3$) 11.40 (s, pz′ CH$_3$), 11.11 (s, pz′ CH$_3$)	—
[Rh{η^4-C$_6$H$_6$C(O)}{HC(pz′)$_3$}][PF$_6$], **10**$^+$[PF$_6$]$^-$	7.72 {s, 1H, *H*C(pz′)$_3$}, 6.74 (dddd, 1H, *J* 7.5, 5, 0.5, 0.5, H^5), 6.57 (dddd, 1H, *J* 7, 5, 0.5, 0.5, H^6), 6.51 (dd, *J* 11, 7, H^3), 6.12 (s, pz′ CH), 6.03 (broad s, pz′ CH), 5.60 (ddd, *J* 11, 2, 1, H^2), 3.93 (ddd, *J* 7, 1, 1, H^7), 3.69 (dd, *J* 7.5, 7, H^4), 2.53 (broad s, pz′ CH$_3$), 2.36 (broad s, pz′ CH$_3$)	201.67 (s, C^{1}O), 157.70 (s, pz′ *C*CH$_3$), 151.04 (s, pz′ *C*CH$_3$), 141.82 (s, C^3), 127.86 (s, C^2), 110.28 (s, pz′ CH), 89.58 (d, $J_{\mathrm{C,Rh}}$ 6, C^5), 85.08 (d, $J_{\mathrm{C,Rh}}$ 6, C^6), 68.00 {s, H*C*(pz′)$_3$}, 44.18 (d, $J_{\mathrm{C,Rh}}$ 17, C^4 or C^7), 34.02 (d, $J_{\mathrm{C,Rh}}$ 17, C^4 or C^7), 14.99 (s, pz′ CH$_3$), 11.31 (s, pz′ CH$_3$), 11.23 (s, pz′ CH$_3$)	—

[a] Chemical shift (δ) in ppm, *J* values in Hz, spectra in CD$_2$Cl$_2$ at 20 °C unless stated otherwise, atom numbering in Scheme 1. [b] At −40 °C. [c] In CD$_3$CN. [d] pz′ CH$_3$, Ph or *C*Ph carbons.

Table 3 Selected bond lengths (Å) and angles (°) for $[Rh(CO)_2\{HC(pz')_3\}][PF_6]$, $\mathbf{1}^+[PF_6]^-$, and $[Rh(CO)(PPh_3)\{HC(pz')_3\}][PF_6]\cdot 2CH_2Cl_2$, $\mathbf{2}^+[PF_6]^-\cdot 2CH_2Cl_2$

	$\mathbf{1a}^{+\,a}$	$\mathbf{1b}^{+\,a}$	$\mathbf{2a}^{+\,b}$	$\mathbf{2b}^{+\,b}$
Rh(1)–N(6)	2.159(2)	2.149(2)	2.106(5)	2.104(5)
Rh(1)–N(4)	2.103(2)	2.119(2)	2.125(6)	2.121(5)
Rh(1)–N(2)	2.431(2)	2.440(2)	3.597(5)	3.614(6)
Rh(1)–C(1)	1.839(3)	1.835(3)	1.821(8)	1.818(7)
Rh(1)–C(2)	1.847(3)	1.848(3)	—	—
Rh(1)–P(1)	—	—	2.266(2)	2.264(2)
N(4)–Rh(1)–N(6)	82.1(1)	84.0(1)	81.3(2)	82.3(2)
N(6)–Rh(1)–C(1)	95.6(1)	94.1(1)	172.0(3)	170.9(3)
C(1)–Rh(1)–C(2)	85.9(1)	84.5(1)	—	—
C(1)–Rh(1)–P(1)	—	—	86.5(2)	86.1(2)
P(1)–Rh(1)–N(4)	—	—	171.9(2)	171.8(2)
C(2)–Rh(1)–N(4)	94.3(1)	95.9(1)	—	—
N(2)–Rh(1)–N(4)	85.5(1)	79.8(1)	—	—
N(2)–Rh(1)–N(6)	77.1(1)	80.6(1)	—	—
N(2)–Rh(1)–C(1)	100.6(1)	105.1(1)	—	—
N(2)–Rh(1)–C(2)	120.8(1)	114.2(1)	—	—
N(4)–Rh(1)–C(1)	172.9(1)	174.4(1)	95.0(3)	95.2(3)
N(6)–Rh(1)–C(2)	161.6(1)	165.1(1)	—	—
N(6)–Rh(1)–P(1)	—	—	98.2(2)	97.7(2)

[a] $\mathbf{1a}^+$ and $\mathbf{1b}^+$ are the two independent molecules of $\mathbf{1}^+$ in the unit cell. [b] $\mathbf{2a}^+$ and $\mathbf{2b}^+$ are the two independent molecules of $\mathbf{2}^+$ in the unit cell.

spectroscopy (Table 2). In addition, the redox chemistry of these complexes was investigated by cyclic voltammetry, and the structure of $[Rh(CO)(PPh_3)\{HC(pz')_3\}][PF_6]\cdot 2CH_2Cl_2$, $\mathbf{2}^+[PF_6]^-\cdot 2CH_2Cl_2$, was determined by X-ray crystallography.

In CH_2Cl_2 each of $\mathbf{2}^+$–$\mathbf{4}^+$ shows only one carbonyl band in the IR spectrum; the carbonyl stretching frequencies of the PPh_3 {and the supposed $P(OPh)_3$} complexes are 20–25 cm^{-1} higher in energy than those of the Tp′ analogues (1978 and 2007 cm^{-1}), reflecting a decrease in electron density at the metal in the cations. As noted above, the dicarbonyl cation $\mathbf{1}^+$ exists as a mixture of the κ^2 and κ^3 isomers in solution. Replacement of a carbonyl ligand by a more bulky, and more electron-donating, ligand would be expected to shift the equilibrium in the direction of κ^2 co-ordination, as found in the Tp′ analogues,[12] so that $\mathbf{2}^+$–$\mathbf{4}^+$ are likely to be κ^2 co-ordinated in solution (as is the case for $\mathbf{2}^+$ in the solid state, see below).

On the NMR spectroscopic timescale all three pyrazolyl rings in cations $\mathbf{2}^+$ and $\mathbf{3}^+$ are equivalent due to fast exchange of the co-ordinated and unco-ordinated rings. In contrast, all three pyrazolyl rings of $\mathbf{4}^+$ are inequivalent, in the room temperature ^1H NMR spectrum and in the ^{13}C NMR spectrum at −40 °C. There is only one major isomer present, but whether this has the A- or B-form (Fig. 1) is unknown. In an A-isomer, all three pyrazolyl rings are likely to remain inequivalent; in a B-isomer, the co-ordinated and unco-ordinated pyrazolyl rings are likely to exchange only slowly due to the steric bulk of the P(*o*-tolyl)$_3$ ligand.

An X-ray structural study showed that, in the solid state at least, $\mathbf{2}^+$ (for which there are two independent molecules in the unit cell) exists in the B-form with the $HC(pz')_3$ ligand κ^2 co-ordinated to square planar rhodium (Fig. 3). As with κ^2 co-ordinated hydrotris(pyrazolyl)borate complexes such as [Rh(CO)LTp′] {L = PPh_3, PCy_3, $P(NMe_2)_3$, P(*m*-tolyl)$_3$ [12] and PMe_3 [21]} and $[Rh(CO)(PMePh_2)L']$ {L′ = hydrotris(3,5-dimethyl-4-chloropyrazolyl)borate}[22] the uncoordinated pyrazolyl ring is orientated *pseudo*-parallel to the rhodium coordination plane. The angle between the rhodium square plane and the plane of the unbound pyrazolyl ring (38.0 and 52.4° for the two independent molecules of $\mathbf{2}^+$) reflects this orientation which results in an average Rh–N$_{\text{apical}}$ separation of 3.61 Å. Overall, the bond lengths and angles of $\mathbf{2}^+$ (Table 3) are remarkably similar to those of [Rh(CO)(PPh$_3$)Tp′].[12]

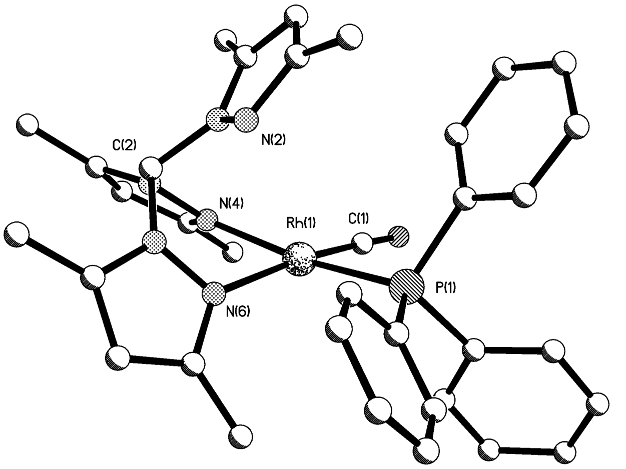

Fig. 3 The molecular structure of the cation of $[Rh(CO)(PPh_3)\{HC(pz')_3\}][PF_6]\cdot 2CH_2Cl_2$, $\mathbf{2}^+[PF_6]^-\cdot 2CH_2Cl_2$. Hydrogen atoms have been omitted for clarity.

The one-electron oxidation of $\mathbf{1}^+$–$\mathbf{4}^+$

The cyclic voltammogram (CV) of $\mathbf{1}^+[PF_6]^-$ in CH_2Cl_2 at a glassy carbon electrode in CH_2Cl_2 shows a one-electron oxidation wave [$(E_p)_{ox}$ = 1.17 V] which is only partially reversible at scan rates between 100 mV s^{-1} and 2 V s^{-1}. Complex $\mathbf{1}^+[PF_6]^-$ is also irreversibly reduced at $(E_p)_{red}$ = −1.55 V with a product wave at $(E_p)_{ox}$ = 0.87 V. The oxidation of [Rh(CO)$_2$Tp′] is better defined, showing a reversible wave at a considerably less positive potential (0.52 V), commensurate with the lower overall charge of the neutral complex.[12]

The CVs of complexes $\mathbf{2}^+[PF_6]^-$ and $\mathbf{3}^+[PF_6]^-$ are also better defined than that of $\mathbf{1}^+[PF_6]^-$, showing reversible one-electron oxidations ($E^{\circ\prime}$ = 0.81 and 0.80 V, respectively). Complex $\mathbf{3}^+[PF_6]^-$ also shows an irreversible second oxidation at $(E_p)_{ox}$ = 1.62 V and an irreversible reduction at $(E_p)_{red}$ = −1.91 V. As with the Tp′ complexes, the peak-to-peak separation for the one-electron oxidation process increases dramatically, and the oxidation peak becomes severely broadened, at a platinum electrode.[12]

The CV of $\mathbf{4}^+[PF_6]^-$ is very different from those of $\mathbf{2}^+[PF_6]^-$ and $\mathbf{3}^+[PF_6]^-$ in showing a poorly defined, irreversible oxidation at $(E_p)_{ox}$ *ca.* 1.30 V with a small product peak at $(E_p)_{red}$ *ca.* 0.65 V. The irreversibility and high positive potential of the oxidation probably arises because the formation of a five-co-ordinate Rh(II) complex (as observed in the formation of the κ^3 cations [Rh(CO)LTp′]$^+$ [12]) is not possible, either because isomerisation on oxidation of $\mathbf{4}^+$ to $\mathbf{4}^{2+}$ is prevented by the steric bulk of the phosphine (if the B-isomer) or because of the *exo*-arrangement of the third pyrazolyl group (if the A-isomer). The complex $[Rh(CO)(PCy_3)Tp^{Ph}]$ {Tp^{Ph} = hydrotris(1-phenylpyrazolyl)borate} is κ^2 co-ordinated as the A-isomer in solution, and the cyclic voltammogram shows a similar irreversible oxidation wave at high potential.[23]

Although attempts to isolate salts of $[Rh(CO)L\{HC(pz')_3\}]^{2+}$ failed [*cf.* the stability of solid [Rh(CO)LTp′][PF$_6$] {L = PPh_3 and $P(NMe_2)_3$} [12]], the Rh(II) dications $[Rh(CO)L\{HC(pz')_3\}]^{2+}$ (L = PPh_3, $\mathbf{2}^{2+}$ and $AsPh_3$, $\mathbf{3}^{2+}$) were generated in the cavity of an ESR spectrometer by oxidising $\mathbf{2}^+[PF_6]^-$ or $\mathbf{3}^+[PF_6]^-$ with $[Fe(\eta\text{-}C_5H_5)(\eta\text{-}C_5H_4COMe)][PF_6]$ at 220 K in dichloromethane–1,2-dichloroethane (1 : 1). The resulting solutions were cooled to 100 or 120 K to obtain the anisotropic ESR spectra, and the temperature was then raised to 290 K for the isotropic spectra. The anisotropic spectrum of $\mathbf{2}^{2+}$ is shown in Fig. 4 and the spectroscopic data for both Rh(II) complexes are given in Table 4.

The anisotropic spectrum of $\mathbf{2}^{2+}$ is similar to that of [Rh(CO)$_2$Tp′]$^+$ [12] in showing coupling to ^{103}Rh and the apical ^{14}N atom in all three *g* components as well as ^{31}P coupling in the high field feature. As with the Rh^{II}Tp′ complexes, the isotropic

Table 4 ESR spectroscopic data for $[Rh(CO)L\{HC(pz')_3\}]^{2+}$ (L = PPh_3, 2^{2+}; $AsPh_3$, 3^{2+})[a]

Complex	g_1	g_2	g_3	g_{ave}	g_{iso}	$A_1(^{103}Rh)$	$A_2(^{103}Rh)$	$A_3(^{103}Rh)$	$A_1(^{14}N)$	$A_2(^{14}N)$	$A_3(^{14}N)$	$A_3(^{31}P)$
2^{2+}	2.272	2.180	1.993	2.148	2.163	22	14	27.3(2)	22	24	28.0(1)	6.4
3^{2+}	2.287	2.170	1.995	2.151	2.171	—	—	21.6(4)	—	—	30.9(3)	—

[a] Anisotropic spectra were computer-simulated; *A*-values for less well-resolved features were analysed by least-squares fits of portions of the spectra to sets of Gaussian absorption lines. Hyperfine couplings in 10^{-4} cm^{-1}.

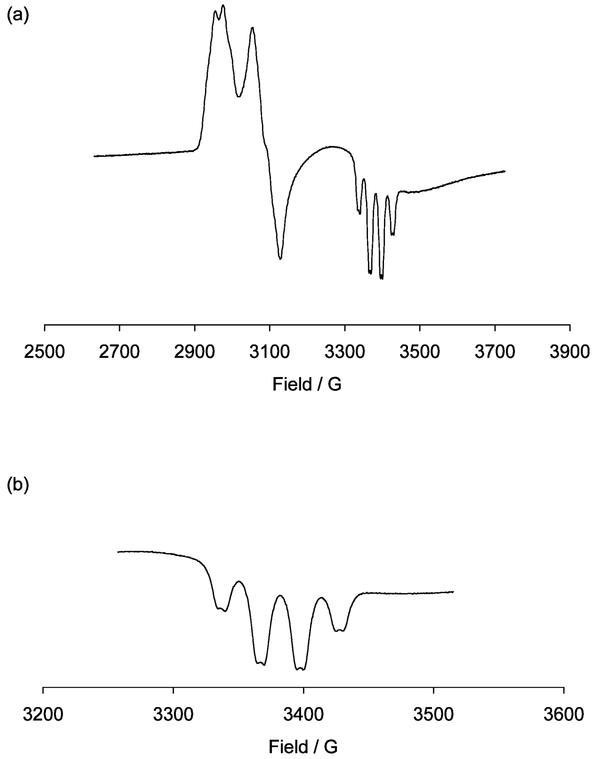

Fig. 4 (a) The anisotropic ESR spectrum of $[Rh(CO)(PPh_3)\{HC(pz')_3\}][PF_6]_2$, $2^{2+}\{[PF_6]^-\}_2$, in 1 : 1 CH_2Cl_2–1,2-dichloroethane at 120 K. The high field component is expanded in (b).

g-value, g_{iso}, is more positive than g_{ave}, perhaps indicating a significant change in the electronic structure with temperature, and possibly due to some departure from square pyramidal geometry leading to admixture of other metal d-orbital character to the SOMO. Further detailed studies of the variable temperature spectra are in progress.

Reactions of $[Rh(CO)_2\{HC(pz')_3\}][PF_6]$, $1^+[PF_6]^-$, with alkynes

In contrast to the cyclopentadienyl complexes $[Rh(CO)_2(\eta\text{-}C_5R_5)]$, which react with alkynes to give a variety of products many of which are multinuclear,[13–18] and $[Rh(CO)_2Tp']$, which is unreactive, $[Rh(CO)_2\{HC(pz')_3\}][PF_6]$, $1^+[PF_6]^-$, and RC≡CR′ give mononuclear products the identities of which depend on R and R′ (Scheme 1).

Synthesis and characterisation of $[Rh(CO)(\eta^2\text{-}PhC{\equiv}CPh)\{HC(pz')_3\}][PF_6]$, $5^+[PF_6]^-$

Heating a thf solution of $1^+[PF_6]^-$ and PhC≡CPh under reflux for five days gave $[Rh(CO)(\eta^2\text{-}PhC{\equiv}CPh)\{HC(pz')_3\}][PF_6]$, $5^+[PF_6]^-$, a rare example of an isolable mononuclear rhodium complex containing both a carbonyl ligand and an η^2-bonded alkyne. (The analogue $[Co(CO)(\eta^2\text{-}PhC{\equiv}CPh)(\eta\text{-}C_5H_5)]$ was detected at −78 °C on UV irradiation of a mixture of $[Co(CO)_2(\eta\text{-}C_5H_5)]$ and PhC≡CPh [24].) By contrast, $[Rh(CO)_2(\eta\text{-}C_5H_5)]$ reacted with PhC≡CPh to give a mixture of C_6Ph_6, the cyclopentadienone complex $[Rh\{\eta^4\text{-}C_4Ph_4C(O)\}(\eta\text{-}C_5H_5)]$, the dinuclear metallacyclopentadiene $[Rh_2(\mu\text{-}C_4Ph_4)(\eta\text{-}C_5H_5)_2]$, and trinuclear $[Rh_3(\mu_3\text{-}CO)(\mu_3\text{-}PhC_2Ph)(\eta\text{-}C_5H_5)_3]$.[18]

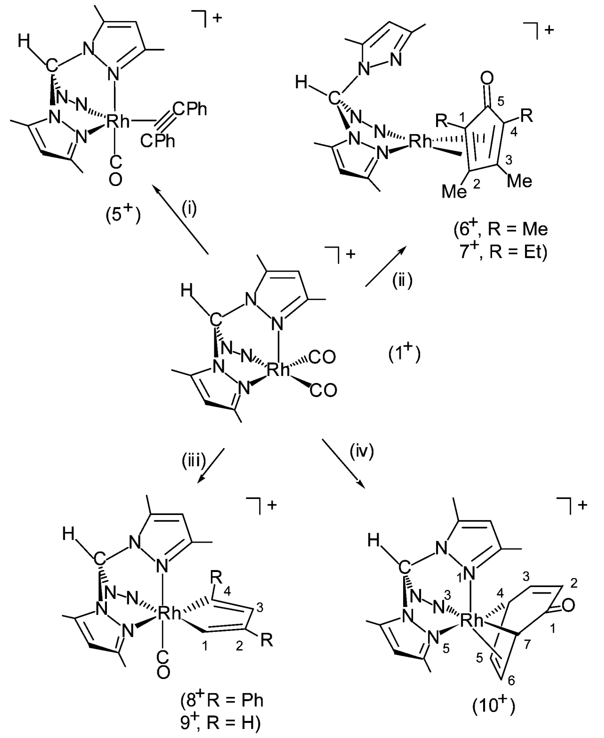

Scheme 1 (i) PhC≡CPh; (ii) MeC≡CR (R = Me or Et); (iii) RC≡CH, R = Ph or H; (iv) HC≡CH. N–N represents the third pyrazolyl ring.

Complex $5^+[PF_6]^-$ was characterised by elemental analysis, by IR spectroscopy (Table 1), showing one terminal carbonyl absorption at 2043 cm^{-1}, and by ^1H and ^{13}C NMR spectroscopy (Table 2) which shows a 2 : 1 ratio for the three pyrazolyl rings. One ^{13}C signal for the alkyne carbon atoms, at 82.5 ppm ($J_{C,Rh}$ = 16 Hz) characteristic of a two-electron alkyne,[25] suggests the alkyne to be disposed such that the C≡C bond is orthogonal to the Rh–C–O linkage (Scheme 1), a suggestion confirmed by an X-ray diffraction study on the solvate $[Rh(CO)(\eta^2\text{-}PhC{\equiv}CPh)\{HC(pz')_3\}][PF_6]\cdot1.5thf$.

The cation 5^+ is shown in Fig. 5 and bond lengths and angles are given in Table 5; general features of the molecular structure are similar to those of $[Rh\{\eta^2\text{-}(MeO_2)C{\equiv}C(CO_2Me)\}(PPh_3)Tp]$ {Tp = hydrotris(pyrazolyl)borate}.[3] The $HC(pz')_3$ ligand is κ^3 coordinated and the C_2Ph_2 ligand is η^2-bonded with the alkyne substituents bent back from the metal by approximately 31°. The geometry at rhodium may be described as trigonal bipyramidal, with the carbonyl axial and the alkyne equatorial, [C(1)–Rh–N(3) = 178.9(3), N(1)–Rh–N(5) = 81.9(2), N(1)–Rh–X(1) = 140.2(3), N(5)–Rh–X(1) = 137.4(3)°, X(1) = midpoint of C(3)–C(4)]. The two equatorial Rh–N bonds *pseudo-trans* to the alkyne [Rh–N(1), 2.200(6); Rh–N(5), 2.185(6)] are somewhat longer than the axial bond *pseudo-trans* to the CO ligand [Rh–N(3), 2.167(7)].

Dissolution of $[Rh(CO)(\eta^2\text{-}PhC{\equiv}CPh)\{HC(pz')_3\}][PF_6]$, $5^+[PF_6]^-$, in either MeCN or Bu^{t}CN at room temperature gave yellow solutions the IR spectra of which show the terminal metal–carbonyl band at 2043 cm^{-1} replaced by a ketonic

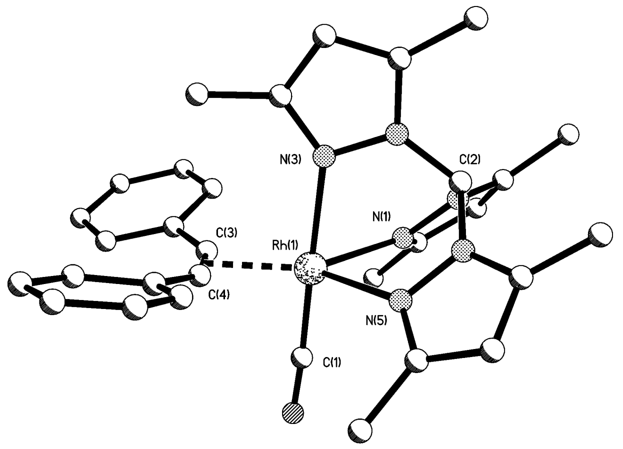

Fig. 5 The molecular structure of the cation of [Rh(CO)(η^2-PhC≡CPh){HC(pz′)$_3$}][PF$_6$]·1.5thf, 5^+[PF$_6$]$^-$·1.5thf. Hydrogen atoms have been omitted for clarity.

carbonyl band, at 1692 and 1700 cm^{-1} respectively. In contrast to the ^{1}H and ^{13}C NMR spectra of **5**$^+$[PF$_6$]$^-$ in CD$_2$Cl$_2$, those in MeCN show three inequivalent pyrazolyl rings. In addition, the ^{13}C spectrum in CD$_3$CN shows a ketonic carbonyl group, at 191.28 ppm, and a *C*Ph carbon resonance at 54.81 ppm.

Further characterisation of this species proved impossible although evaporating the MeCN or Bu^{t}CN solutions to dryness and dissolving the residues in CH$_2$Cl$_2$ resulted in the reappearance of the IR band at 2043 cm^{-1}, *i.e.* in the reformation of **5**$^+$. By contrast, when **5**$^+$[PF$_6$]$^-$ was heated under reflux in MeCN, a yellow solution {with ν(CO) at 1713 cm^{-1}} was formed from which **5**$^+$[PF$_6$]$^-$ could not be recovered; the complex ^{1}H NMR spectrum of the product, in CD$_2$Cl$_2$, indicated a mixture of species.

Table 5 Selected bond lengths (Å) and angles (°) for [Rh(CO)(η^2-C$_2$Ph$_2$){HC(pz′)$_3$}][PF$_6$]·1.5thf, **5**$^+$[PF$_6$]$^-$·1.5thf

Rh(1)–N(1)	2.185(6)	Rh(1)–C(3)	2.068(8)
Rh(1)–N(3)	2.167(7)	Rh(1)–C(4)	2.061(9)
Rh(1)–N(5)	2.200(6)	C(3)–C(4)	1.251(11)
Rh(1)–C(1)	1.796(9)	Rh(1)–X(1)	1.967
C(1)–Rh(1)–C(4)	87.1(4)	C(3)–Rh(1)–N(5)	155.0(3)
C(1)–Rh(1)–C(3)	86.6(3)	N(3)–Rh(1)–N(5)	84.4(3)
C(1)–Rh(1)–N(3)	178.9(3)	N(1)–Rh(1)–N(5)	81.9(2)
C(3)–Rh(1)–N(3)	94.5(3)	C(3)–C(4)–C(31)	150.3(10)
C(4)–Rh(1)–N(3)	93.7(3)	C(4)–C(3)–C(21)	147.8(9)
C(1)–Rh(1)–N(1)	96.9(3)	N(1)–Rh(1)–X(1)[a]	140.2
C(1)–Rh(1)–N(5)	94.6(3)	N(5)–Rh(1)–X(1)[a]	137.4
N(5)–Rh(1)–C(4)	119.8(3)		

[a] X(1) = midpoint of C(3)–C(4).

Synthesis and characterisation of [Rh{η^4-C$_4$Me$_2$R$_2$C(O)}{HC(pz′)$_3$}][PF$_6$] (R = Me, 6^+[PF$_6$]$^-$ or Et, 7^+[PF$_6$]$^-$)

The reaction of **1**$^+$ with MeC≡CMe in CH$_2$Cl$_2$ at room temperature gave the red–pink cyclopentadienone complex [Rh{η^4-C$_4$Me$_4$C(O)}{HC(pz′)$_3$}][PF$_6$], **6**$^+$[PF$_6$]$^-$, [ν(CO) = 1667 cm^{-1}] in which two alkynes and a carbonyl ligand are linked. Small quantities of a second, yellow product, with ν(CO) = 2046 cm^{-1}, remained in solution after precipitation of **6**$^+$[PF$_6$]$^-$ from CH$_2$Cl$_2$ with *n*-hexane. Though not further characterised, this complex is most likely the η^2-alkyne complex [Rh(CO)(η^2-MeC≡CMe){HC(pz′)$_3$}][PF$_6$] on the basis of the close similarity between its carbonyl stretching frequency and that of **5**$^+$[PF$_6$]$^-$ [ν(CO) = 2043 cm^{-1}]. (By comparison, the reaction between [Rh(CO)$_2$(η-C$_5$H$_5$)] and MeC≡CMe gave a mixture of the cyclopentadienone complex [Rh{η^4-C$_4$Me$_4$C(O)}(η-C$_5$H$_5$)] and the duroquinone complex [Rh(η^4-C$_6$Me$_4$O$_2$-*p*)(η-C$_5$H$_5$)],[14] but with [Rh(CO)$_2$(η-C$_5$Me$_5$)] the major product was [Rh{η^4-C$_4$Me$_4$C(O)}(η-C$_5$Me$_5$)].[15])

The ^{1}H NMR spectrum of **6**$^+$[PF$_6$]$^-$ shows two singlet resonances for the two inequivalent pairs of methyl groups on the cyclopentadienone ring. Only one resonance is observed for the pyrazolyl ring protons and only two singlets for the methyl groups in the 3- and 5-positions of the rings. Similarly, the ^{13}C NMR spectrum shows only one signal for each of the two different pyrazolyl ring methyls and one for the ring protons; the diene carbons show couplings of 9 and 12 Hz to the rhodium atom. Although the NMR spectra imply that the three pyrazolyl rings are equivalent, an X-ray structural study revealed that this equivalence is most likely due to a fluxional process in which two bound and one unbound pyrazolyl groups of a κ^2 ligand interconvert.

The molecular structure of **6**$^+$ is shown in Fig. 6 with important bond lengths and angles given in Table 6. If the rhodium–alkene bonds are defined as those from rhodium to the centres of the C=C bonds [*i.e.* X(1) = midpoint of C(18)–C(19), X(2) = midpoint of C(20)–C(21)], then the geometry about rhodium is approximately square planar. The HC(pz′)$_3$ ligand is κ^2 co-ordinated with the uncoordinated pyrazolyl ring orientated *pseudo*-parallel to the rhodium coordination plane; the angle between the rhodium square plane and that of the unbound pyrazolyl ring is 60.9°. The dienone ring is orientated such that the oxygen atom of the ketone group is located at only 3.37 Å from the centre of the unbound pyrazolyl ring.

There are two extremes for the bonding of a metal to a 1,3-diene unit, as shown in Fig. 7. In Fig. 7(a) the metal is

Table 6 Selected bond lengths (Å) and angles (°) for [Rh{η^4-C$_4$Me$_4$C(O)}{HC(pz′)$_3$}][PF$_6$], **6**$^+$[PF$_6$]$^-$, and [Rh{η^4-C$_4$Me$_2$Et$_2$C(O)}{HC(pz′)$_3$}][PF$_6$]·H$_2$O, **7**$^+$[PF$_6$]$^-$·H$_2$O

	6	7		6	7
Rh(1)–N(4)	2.143(4)	2.135(5)	Rh(1)–X(1)	2.040	2.029
Rh(1)–N(6)	2.155(4)	2.118(7)	Rh(1)–X(2)	2.018	2.030
Rh(1) ··· N(2)	3.484(4)	3.570(6)	C(18)–C(19)	1.416(7)	1.403(9)
Rh(1)–C(18)	2.173(5)	2.142(6)	C(19)–C(20)	1.453(7)	1.448(9)
Rh(1)–C(19)	2.147(5)	2.151(7)	C(20)–C(21)	1.420(7)	1.407(10)
Rh(1)–C(20)	2.133(5)	2.141(6)	C(21)–C(17)	1.465(7)	1.468(9)
Rh(1)–C(21)	2.145(5)	2.156(8)	C(18)–C(17)	1.490(7)	1.486(8)
Rh(1) ··· C(17)	2.416(5)	2.348(6)	C(17)–O(1)	1.230(6)	1.237(7)
N(4)–Rh(1)–N(6)	82.3(2)	83.7(2)	C(19)–C(20)–C(21)	108.2(4)	107.8(6)
N(4)–Rh(1)–X(1)[a]	163.0	165.3	C(20)–C(21)–C(17)	108.6(4)	109.3(6)
N(4)–Rh(1)–X(2)[a]	108.6	110.9	C(21)–C(17)–C(18)	103.7(4)	103.9(5)
N(6)–Rh(1)–X(1)[a]	111.9	109.5	C(17)–C(18)–C(19)	108.4(4)	108.3(5)
N(6)–Rh(1)–X(2)[a]	163.3	164.5	C(21)–C(17)–O(1)	127.9(5)	128.4(6)
C(18)–C(19)–C(20)	107.7(4)	108.6(5)	C(18)–C(17)–O(1)	128.2(5)	127.4(6)

[a] X(1) = midpoint of C(18)–C(19), X(2) = midpoint of C(20)–C(21).

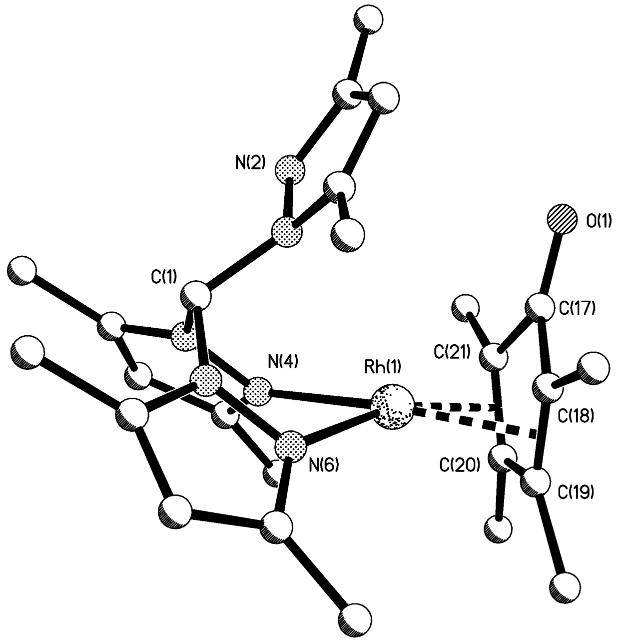

Fig. 6 The molecular structure of the cation of [Rh{η^4-C_4Me_4-C(O)}{HC(pz′)$_3$}][PF_6], $6^+[PF_6]^-$. Hydrogen atoms have been omitted for clarity.

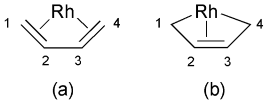

Fig. 7 The two extremes of bonding of a butadiene fragment to a metal, (a) as an η^4-diene, and (b) as a metallacyclopentene.

coordinated to two independent alkene units, C(1)–C(2) and C(3)–C(4), and in Fig. 7(b) to an alkene, C(2)–C(3), and the two terminal carbon atoms, C(1) and C(4). The carbon–carbon bond lengths in the $C_4Me_4C(O)$ ring of 6^+ [C(18)–C(19), 1.416(7); C(19)–C(20), 1.453(7); C(20)–C(21), 1.420(7) Å] suggest that the bonding is closer to that shown in Fig. 7(a). The planarity of the dienone ring (fold angle at C(18) ··· C(21) 3.9°) is also consistent with this bonding mode, *i.e.* with sp^2 hybridisation at carbons C(19) and C(21).

The reaction of 1^+ with MeC≡CEt in CH_2Cl_2 at room temperature also gave a red solid the elemental analysis and IR spectrum [ν(CO) = 1661 cm^{-1}] of which were consistent with the formation of an analogue of 6^+, namely [Rh{η^4-C_4Me_2-$Et_2C(O)$}{HC(pz′)$_3$}][PF_6], $7^+[PF_6]^-$. However, the ^{1}H and ^{13}C NMR spectra were complex, suggesting only that a mixture of all three possible cyclopentadienone isomers was formed, *i.e.* the symmetric head-to-head isomers (a) and (b) and the asymmetric head-to-tail isomer (c) shown in Fig. 8. Slow diffusion of a concentrated CH_2Cl_2 solution of the red solid into *n*-hexane at −10° gave red crystals of $7^+[PF_6]^-$, an X-ray study on which (Fig. 9, Table 6) showed a very similar structure to that of $6^+[PF_6]^-$. In the case of $7^+[PF_6]^-$, however, the two asymmetric alkyne units are linked head-to-head and the two CEt termini are bound to the ketonic CO group, *i.e.* as in Fig. 8(a) (R_1 = Et, R_2 = Me). Again, the dienone ring is orientated such that the oxygen atom of the ketone group is close to the centre of the unbound pyrazolyl ring (at *ca.* 3.26 Å).

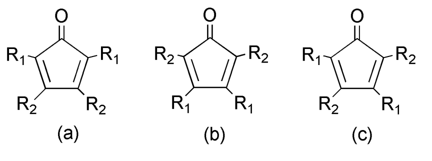

Fig. 8 Head-to-head [(a) and (b)] and head-to-tail (c) isomers of a cyclopentadienone.

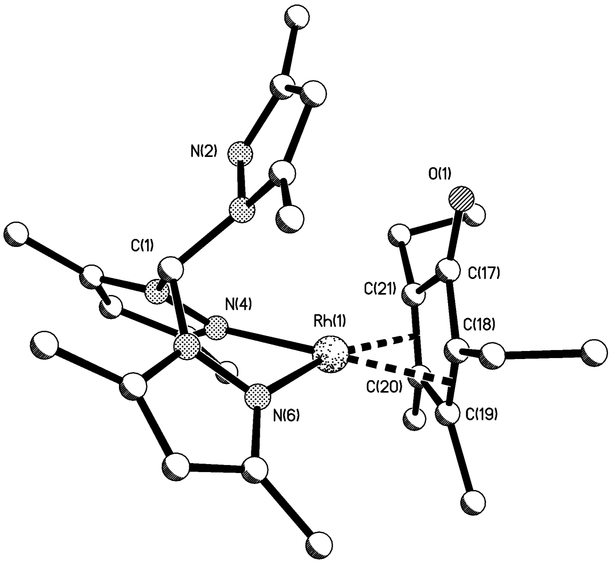

Fig. 9 The molecular structure of the cation of [Rh{η^4-C_4Me_2-$Et_2C(O)$}{HC(pz′)$_3$}][PF_6]·H_2O, $7^+[PF_6]^-$·H_2O. Hydrogen atoms have been omitted for clarity.

Reactions with terminal alkynes: synthesis and characterisation of [Rh(CO)(η^1:$\eta^{1\prime}$-$C_4R_2R'_2$){HC(pz′)$_3$}][PF_6] (R = H, R′ = Ph, $8^+[PF_6]^-$; R = R′ = H, $9^+[PF_6]^-$) and [Rh{η^4-$C_6H_6C(O)$}-{HC(pz′)$_3$}][PF_6], $10^+[PF_6]^-$

The terminal alkynes HC≡CPh and HC≡CH react very differently with 1^+ than do internal alkynes. Thus, HC≡CPh and $1^+[PF_6]^-$ in CH_2Cl_2 gave the cream metallacyclopentadiene complex [Rh(CO)(η^1:$\eta^{1\prime}$-CHCPhCHCPh){HC(pz′)$_3$}][PF_6], $8^+[PF_6]^-$, whereas HC≡CH gave a mixture of the yellow analogue [Rh(CO)(η^1:$\eta^{1\prime}$-C_4H_4){HC(pz′)$_3$}][PF_6], $9^+[PF_6]^-$, plus small amounts of the orange cycloheptatrienone (tropone) complex [Rh{η^4-$C_6H_6C(O)$}{HC(pz′)$_3$}][PF_6], $10^+[PF_6]^-$, an analogue of which was isolated from the reaction between [Rh(CO)$_2$Cp] and the diyne MeC≡CC≡CMe.[16]

The IR spectra of complexes $8^+[PF_6]^-$ and $9^+[PF_6]^-$ (Table 1) each show a peak for the terminal carbonyl ligand (2083 and 2080 cm^{-1}, respectively), but at higher wavenumber than the Rh(I) complex, $5^+[PF_6]^-$, (2043 cm^{-1}), consistent with the presence of the higher oxidation state Rh(III).

The structure of cation 9^+ (Fig. 10, Table 7) is similar to that of [Ir(η-C_2H_4)(η^1:$\eta^{1\prime}$-CRCRCRCR)Tp] (R = CO_2Me),[26] with an octahedral metal centre κ^3-bound to the tris(3,5-dimethylpyrazolyl)methane ligand. The Rh–N$_{\text{pyrazolyl}}$ bond *trans* to the carbonyl ligand [Rh–N(2) = 2.110(3)] is shorter than those *trans* to the carbon atoms of the metallacyclopentadiene ring [Rh–N(6) = 2.185(4), Rh–N(4) = 2.194(4) Å]. The two phenyl rings are positioned asymmetrically on the five-membered metallacycle such that the two alkynes are linked head-to-tail (*cf.* head-to-head linkage in the cyclopentadienone complex 7^+).

In agreement with the structural study, all three pyrazolyl rings in 8^+ are inequivalent in the ^{1}H and ^{13}C–{^{1}H} NMR spectra (Table 2). In the ^{1}H NMR spectrum the phenyl proton signals partly obscure those for H^1 and H^3 (see Scheme 1 for numbering), and C^1 and C^3 are amongst the twelve ^{13}C NMR signals between 160 and 138 ppm. However, DEPT NMR spectroscopy allowed the C^1 and C^3 signals to be assigned, at 139.78 and 143.96 ppm (with coupling to rhodium of 26 and 2 Hz, respectively), and ^{1}H/^{13}C correlated NMR spectroscopy then enabled the peaks due to H^1 and H^3 to be located, one at 7.85 ppm and the other within a 3H multiplet between 6.91 and 6.87 ppm.

In cation 9^+, which contains a symmetrical metallacyclopentadiene ring, the pyrazolyl groups are observed in a 2 : 1 ratio. In addition, the ^{1}H signals for the protons of the C_4H_4Rh ring were more easily identified (at 7.52 and 6.51 ppm for H^1/H^4

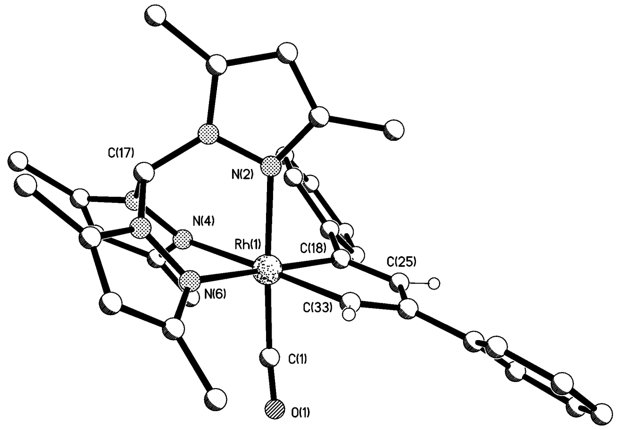

Fig. 10 The molecular structure of the cation of [Rh(CO)(η^1:η$^{1'}$-CHCPhCHCPh){HC(pz′)$_3$}][PF$_6$]·2CH$_2$Cl$_2$, **8**$^+$[PF$_6$]$^-$·2CH$_2$Cl$_2$. Most hydrogen atoms have been omitted for clarity.

Table 7 Selected bond lengths (Å) and angles (°) for [Rh(CO)(η^1:η$^{1'}$-CHCPhCHCPh){HC(pz′)$_3$}][PF$_6$]·2CH$_2$Cl$_2$, **8**$^+$[PF$_6$]$^-$·2CH$_2$Cl$_2$

Rh(1)–N(4)	2.194(4)	Rh(1)–C(33)	2.033(4)
Rh(1)–N(6)	2.185(4)	C(18)–C(25)	1.347(6)
Rh(1)–N(2)	2.110(3)	C(25)–C(26)	1.458(6)
Rh(1)–C(1)	1.861(5)	C(26)–C(33)	1.346(6)
Rh(1)–C(18)	2.061(4)		
C(1)–Rh(1)–N(2)	176.7(2)	C(18)–Rh(1)–N(6)	174.0(2)
C(1)–Rh(1)–N(6)	98.3(2)	C(33)–Rh(1)–N(2)	96.7(2)
C(1)–Rh(1)–N(4)	97.4(2)	C(33)–Rh(1)–N(6)	95.0(2)
C(1)–Rh(1)–C(18)	83.4(2)	N(2)–Rh(1)–N(6)	84.3(1)
C(1)–Rh(1)–C(33)	81.1(2)	N(2)–Rh(1)–N(4)	84.9(1)
C(18)–Rh(1)–C(33)	79.6(2)	N(4)–Rh(1)–N(6)	84.2(1)
C(18)–Rh(1)–N(2)	93.9(2)		

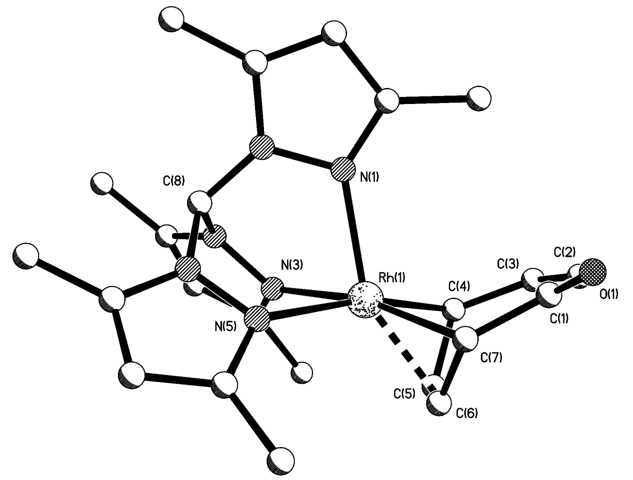

Fig. 11 The molecular structure of the cation of [Rh{η^4-C$_6$H$_6$C(O)-}{HC(pz′)$_3$}][PF$_6$], **10**$^+$[PF$_6$]$^-$. Hydrogen atoms have been omitted for clarity.

Table 8 Selected bond lengths (Å) and angles (°) for [Rh{η^4–C$_6$H$_6$C(O)}{HC(pz′)$_3$}][PF$_6$], **10**$^+$[PF$_6$]$^-$

Rh(1)–N(1)	2.175(8)	C(1)–C(2)	1.439(16)
Rh(1)–N(3)	2.159(8)	C(2)–C(3)	1.352(17)
Rh(1)–N(5)	2.200(9)	C(3)–C(4)	1.465(16)
Rh(1)–C(4)	2.116(11)	C(4)–C(5)	1.433(16)
Rh(1)–C(5)	2.105(11)	C(5)–C(6)	1.391(16)
Rh(1)–C(6)	2.087(10)	C(6)–C(7)	1.423(15)
Rh(1)–C(7)	2.118(10)	C(7)–C(1)	1.475(15)
C(1)–O(1)	1.225(13)		
N(3)–Rh(1)–N(5)	81.4(3)	N(1)–Rh(1)–N(5)	84.2(3)
N(3)–Rh(1)–C(4)	95.7(4)	N(1)–Rh(1)–C(4)	108.3(4)
C(4)–Rh(1)–C(7)	81.8(4)	N(1)–Rh(1)–C(7)	107.5(3)
C(7)–Rh(1)–N(5)	98.4(4)	N(5)–Rh(1)–C(4)	166.9(4)
N(1)–Rh(1)–N(3)	84.2(3)	N(3)–Rh(1)–C(7)	168.2(4)

and H^2/H^3, respectively), ^{1}H/^{13}C correlated NMR spectroscopy then showing that C^1/C^4 and C^2/C^3 occur at 145.47 and 147.65 ppm, respectively in the ^{13}C NMR spectrum.

The IR spectrum of the η^4-cycloheptatrienone (tropone) complex **10**$^+$[PF$_6$]$^-$ shows not only a ketonic peak [*ν*(CO) (CH$_2$Cl$_2$, 1640 cm^{-1}; Nujol, 1635 cm^{-1})], but also a *ν*(C=C) absorption (CH$_2$Cl$_2$, 1616 cm^{-1}; Nujol, 1609 cm^{-1}), similar to those of [Fe(CO)$_3${η^4-C$_6$H$_6$C(O)}] (1637 and 1613 cm^{-1}, respectively)[27] and the molecular structure of cation **10**$^+$ (Fig. 11, Table 8) is also similar to that of the iron compound.[28]

Unlike the cyclopentadienone complexes **6**$^+$[PF$_6$]$^-$ and **7**$^+$[PF$_6$]$^-$, the cycloheptatrienone derivative **10**$^+$[PF$_6$]$^-$has a κ^3 co-ordinated HC(pz′)$_3$ ligand, and a very different bonding mode for the diene unit. Thus, in cation **10**$^+$ the C–C bond distances [C(4)–C(5), 1.433(16); C(5)–C(6), 1.391(16); C(6)–C(7), 1.423(15) Å] suggest dominance of the bonding mode shown in Fig. 7(b), *i.e.* with two Rh–C σ-bonds and one Rh–alkene interaction; the fold angle at C(4) ··· C(7) (49.8°) is also consistent with σ-bonds between sp^3-hybridised carbon atoms C^4 and C^7 and the metal. The bonding between the metal and cyclopentadienone shows, therefore, that the κ^3 coordinated HC(pz′)$_3$ ligand acts as a better net donor than the κ^2 form in **6**$^+$ and **7**$^+$, with consequently enhanced donation from metal to diene.

Finally, the unbound part of the cycloheptatrienone ring, C(1)–C(3), is orientated away from the third (bound) pyrazolyl ring in **10**$^+$, *cf.* the orientation of the ketonic carbonyl group of the cyclopentadienone ring of **6**$^+$ (towards the third, unbound, pyrazolyl ring), presumably for steric reasons.

The ^{1}H NMR spectrum of **10**$^+$[PF$_6$]$^-$ shows six signals for the protons of the η^4-C$_6$H$_6$O ring, assigned by ^{1}H/^{1}H correlated spectroscopy. The ^{13}C–{^{1}H} NMR spectrum shows seven peaks for C^1–C^7. The peak above 200 ppm is characteristic of a ketonic carbon atom (C^1) and the peaks at 127.86 and 141.82 ppm have been assigned as C^2 and C^3 by comparison of the chemical shifts with those of the α,β-unsaturated ketone 2,3-cyclohexenone (C^2, 130 ppm; C^3, 151).[29] The C^5 and C^6 signals were assigned by ^{1}H/^{13}C correlated NMR spectroscopy which shows coupling of protons H^5 and H^6 to signals at 89.58 (C^5) and 85.08 (C^6) ppm, respectively. The rhodium couplings are larger for the σ-bound carbon atoms C^4 and C^7 (17 Hz) than for C^5 and C^6 (6 Hz).

Conclusion

The dicarbonyl [Rh(CO)$_2${HC(pz′)$_3$}][PF$_6$], **1**$^+$[PF$_6$]$^-$, easily prepared in high yield, provides an excellent route into rhodium tris(3,5-dimethylpyrazolyl)methane chemistry. The cation reacts more readily than the Tp′ analogue [Rh(CO)$_2$Tp′], undergoing carbonyl substitution to give [Rh(CO)L{HC-(pz′)$_3$}][PF$_6$] with Lewis bases and giving a range of products with alkynes, including mononuclear cyclopentadienone, metallacyclopentadiene and cycloheptatrienone complexes.

Experimental

The preparation, purification and reactions of the complexes described were carried out under an atmosphere of dry nitrogen using dried, distilled and deoxygenated solvents; reactions were monitored by IR spectroscopy where necessary. Percentage yields are based upon the rhodium-containing starting materials. Unless stated otherwise, complexes (i) were purified by dissolution in CH$_2$Cl$_2$, filtration of the solution through Celite, addition of *n*-hexane to the filtrate and reduction of the volume of the mixture *in vacuo* to induce precipitation, and (ii) are stable under nitrogen and dissolve in polar solvents such as CH$_2$Cl$_2$ and thf.

The compounds $[\{Rh(CO)_2(\mu\text{-}Cl)\}_2]$,[30] and $[Fe(\eta\text{-}C_5H_5)(\eta\text{-}C_5H_4COMe)][PF_6]$[31] were prepared by published methods. The ligand $HC(pz')_3$ was synthesised by a combination of two literature preparations.[32,33]

IR spectra were recorded on a Nicolet 5ZDX FT spectrometer. NMR spectra were recorded on a JEOL λ300 spectrometer with $SiMe_4$ as an internal standard for ^1H and ^{13}C spectra, and external H_3PO_4 as a ^{31}P standard. X-band ESR spectra were recorded on a Bruker ESP300 spectrometer equipped with a Bruker variable temperature accessory and a Hewlett-Packard 5350B microwave frequency counter. The field calibration was checked by measuring the resonance of the dpph radical before each series of spectra.

Electrochemical studies were carried out in CH_2Cl_2 using an EG&G model 273A potentiostat in conjunction with a three-electrode cell. The auxiliary electrode was a platinum wire and the working electrode a glassy-carbon disc (3.0 mm diameter). The reference was an aqueous saturated calomel electrode separated from the test solution by a fine porosity frit and an agar bridge saturated with KCl. Solutions were 1.0×10^{-3} mol dm^{-3} in the test compound and 0.1 mol dm^{-3} in $[NBu^n_4][PF_6]$ as the supporting electrolyte. Under the conditions used, $E^{\circ\prime}$ for the one-electron oxidation of $[Fe(\eta\text{-}C_5H_5)_2]$ or $[Fe(\eta\text{-}C_5H_4COMe)_2]$, added to the test solutions as internal calibrants, is 0.47 and 0.97 V, respectively. Microanalyses were carried out by the staff of the Microanalysis Service of the School of Chemistry, University of Bristol.

Syntheses

Tris(3,5-dimethylpyrazolyl)methane, $HC(pz')_3$. Solid K_2CO_3 (49.8 g, 360 mmol) was dried by heating *in vacuo*. After cooling the sample to room temperature, 3,5-dimethylpyrazole (6.92 g, 72 mmol), $[NBu^n_4][HSO_4]$ (1.22 g, 3.6 mmol) and $CHCl_3$ (75 cm^3) were added, and the mixture was heated under reflux for 24 h. The brown mixture was filtered and the solid washed with boiling $CHCl_3$ (3 × 50 cm^3). The filtrate and washings were evaporated to dryness *in vacuo* to leave a brown oil which was dissolved in CH_2Cl_2 (25 cm^3), adsorbed onto silica and applied (in air) to a water-cooled silica–*n*-hexane chromatography column (30–40 cm long). The colourless product was eluted, as the second eluate, by using a diethyl ether–*n*-hexane mixture and slowly changing the ratio of the two solvents from 1 : 4 to 1 : 1. The fractions containing only the desired product were evaporated to low volume *in vacuo* and *n*-hexane was added to give a white solid and bright yellow mother liquors. The solid was collected, washed with *n*-hexane (4 × 20 cm^3) and dried *in vacuo* for 24 h, yield 2.9 g (41%).

$[Rh(CO)_2\{HC(pz')_3\}][PF_6]$, $1^+[PF_6]^-$. A solution of $[\{Rh(CO)_2(\mu\text{-}Cl)\}_2]$ (0.70 g, 1.80 mmol) and $HC(pz')_3$ (1.06 g, 3.60 mmol) in CH_2Cl_2 (100 cm^3) was stirred for 30 min before $Tl[PF_6]$ (1.47 g, 3.78 mmol) was added. After 5 h the solution was filtered through Celite, concentrated *in vacuo* and layered with *n*-hexane. Slowly stirring the layered mixture then gave a yellow, crystalline precipitate which was dried *in vacuo* for 24 h, yield 2.04 g (94%).

$[Rh(CO)(PPh_3)\{HC(pz')_3\}][PF_6]\cdot CH_2Cl_2$, $2^+[PF_6]^-\cdot CH_2Cl_2$. A solution of $[Rh(CO)_2\{HC(pz')_3\}][PF_6]$, $1^+[PF_6]^-$, (100 mg, 0.17 mmol) and PPh_3 (44 mg, 0.17 mmol) in CH_2Cl_2 (10 cm^3) was stirred for 5 min before *n*-hexane was added to precipitate a yellow microcrystalline solid. A concentrated CH_2Cl_2 solution of the solid was allowed to diffuse slowly into *n*-hexane at −10 °C to give yellow crystals, yield 90 mg (64%).

$[Rh(CO)(AsPh_3)\{HC(pz')_3\}][PF_6]\cdot CH_2Cl_2$, $3^+[PF_6]^-\cdot CH_2Cl_2$. A solution of $[Rh(CO)_2\{HC(pz')_3\}][PF_6]$, $1^+[PF_6]^-$ (200 mg, 0.33 mmol), and $AsPh_3$ (407 mg, 1.33 mmol) in CH_2Cl_2 (10 cm^3) was stirred for 4 d and then filtered through Celite. The resulting yellow solution was evaporated to smaller volume *in vacuo*, and then toluene was added to precipitate a bright yellow solid which was dried *in vacuo* for 24 h. The product was dissolved in CH_2Cl_2, layered with *n*-hexane, and then slowly stirred to give a yellow crystalline solid, yield 230 mg (72%).

$[Rh(CO)\{P(o\text{-}tolyl)_3\}\{HC(pz')_3\}][PF_6]\cdot 0.5CH_2Cl_2$, $4^+[PF_6]^-\cdot 0.5CH_2Cl_2$. A solution of $[Rh(CO)_2\{HC(pz')_3\}][PF_6]$, $1^+[PF_6]^-$ (200 mg, 0.33 mmol), and $P(o\text{-}tolyl)_3$ (202 mg, 0.66 mmol) in thf (40 cm^3) was heated under reflux for 2 d and then evaporated to dryness *in vacuo*. The residue was dissolved in CH_2Cl_2 (20 cm^3) and then *n*-hexane (*ca.* 30 cm^3) was added to give a grey precipitate which was removed by filtration and discarded. The volume of the filtrate was reduced *in vacuo* until a yellow precipitate started to form which was again removed by filtration and discarded. Addition of *n*-hexane to the filtrate then gave the product as a bright yellow solid, yield 90 mg (29%).

$[Rh(CO)(\eta^2\text{-}PhC{\equiv}CPh)\{HC(pz')_3\}][PF_6]\cdot CH_2Cl_2$, $5^+[PF_6]^-\cdot CH_2Cl_2$. A solution of $[Rh(CO)_2\{HC(pz')_3\}][PF_6]$, $1^+[PF_6]^-$ (400 mg, 0.66 mmol), and $PhC{\equiv}CPh$ (124 mg, 0.70 mmol) in thf (40 cm^3) was heated under reflux for 5 d and then filtered through Celite and evaporated to dryness *in vacuo*. The product was washed with diethyl ether and then purified to give a fawn precipitate which was collected, washed with diethyl ether and dried *in vacuo*, yield 300 mg (54%).

$[Rh\{\eta^4\text{-}C_4Me_4C(O)\}\{HC(pz')_3\}][PF_6]$, $6^+[PF_6]^-$. A solution of $[Rh(CO)_2\{HC(pz')_3\}][PF_6]$, $1^+[PF_6]^-$ (100 mg, 0.17 mmol), and $MeC{\equiv}CMe$ (150 μl, 1.92 mmol) in CH_2Cl_2 (20 cm^3) was stirred for 2 d and then allowed to diffuse slowly into *n*-hexane at −10 °C to give a salmon-pink solid. A concentrated CH_2Cl_2 solution of the solid was allowed to diffuse slowly into diethyl ether at room temperature to give dark red crystals which were dried *in vacuo*, yield 67 mg (59%).

A similar reaction with $MeC{\equiv}CEt$ gave a mixture of isomers of $[Rh\{\eta^4\text{-}C_4Me_2Et_2C(O)\}\{HC(pz')_3\}][PF_6]$, $7^+[PF_6]^-$.

$[Rh(\eta^1{:}\eta^{1\prime}\text{-}CHCPhCHCPh)(CO)\{HC(pz')_3\}][PF_6]$, $8^+[PF_6]^-$. A solution of $[Rh(CO)_2\{HC(pz')_3\}][PF_6]$, $1^+[PF_6]^-$ (100 mg, 0.17 mmol), and $HC{\equiv}CPh$ (200 μl, 1.82 mmol) in CH_2Cl_2 (10 cm^3) was stirred for 3 h and then *n*-hexane was added to precipitate a pale yellow solid. Purification gave a cream solid which was dried *in vacuo*, yield 112 mg (90%).

$[Rh(CO)(\eta^1{:}\eta^{1\prime}\text{-}C_4H_4)\{HC(pz')_3\}][PF_6]$, $9^+[PF_6]^-$, and $[Rh\{\eta^4\text{-}C_6H_6C(O)\}\{HC(pz')_3\}][PF_6]$, $10^+[PF_6]^-$. Gaseous ethyne was slowly bubbled through a solution of $[Rh(CO)_2\{HC(pz')_3\}][PF_6]$, $1^+[PF_6]^-$ (150 mg, 0.25 mmol), in CH_2Cl_2 (75 cm^3) for 8 h to give a bright yellow solution which was evaporated to dryness *in vacuo*. The oily orange residue was dissolved in CH_2Cl_2 before diethyl ether was added to give small amounts of an orange precipitate of $[Rh\{\eta^4\text{-}C_6H_6C(O)\}\{HC(pz')_3\}][PF_6]$, $10^+[PF_6]^-$. The mother liquors were then concentrated *in vacuo*, and diethyl ether was added to precipitate pale yellow $[Rh(CO)(\eta^1{:}\eta^{1\prime}\text{-}C_4H_4)\{HC(pz')_3\}][PF_6]$, $9^+[PF_6]^-$, which was dried *in vacuo*, yield 65 mg (42%).

Crystal structure determinations of $[Rh(CO)_2\{HC(pz')_3\}][PF_6]$, $1^+[PF_6]^-$, $[Rh(CO)(PPh_3)\{HC(pz')_3\}][PF_6]\cdot 2CH_2Cl_2$, $2^+[PF_6]^-\cdot 2CH_2Cl_2$, $[Rh(CO)(\eta^2\text{-}PhC{\equiv}CPh)\{HC(pz')_3\}][PF_6]\cdot 1.5thf$, $5^+[PF_6]^-\cdot 1.5thf$, $[Rh\{\eta^4\text{-}C_4Me_4C(O)\}\{HC(pz')_3\}][PF_6]$, $6^+[PF_6]^-$, $[Rh\{\eta^4\text{-}C_4Me_2Et_2C(O)\}\{HC(pz')_3\}][PF_6]$, $7^+[PF_6]^-\cdot H_2O$, $[Rh(CO)(\eta^1{:}\eta^{1\prime}\text{-}CHCPhCHCPh)\{HC(pz')_3\}][PF_6]\cdot 2CH_2Cl_2$, $8^+[PF_6]^-\cdot 2CH_2Cl_2$, and $[Rh\{\eta^4\text{-}C_6H_6C(O)\}\{HC(pz')_3\}][PF_6]$, $10^+[PF_6]^-$. Crystals suitable for X-ray diffraction study were grown as follows: $1^+[PF_6]^-$, slow diffusion of a concentrated CH_2Cl_2 solution of the complex into *n*-hexane at room temperature; $2^+[PF_6]^-\cdot 2CH_2Cl_2$, $7^+[PF_6]^-\cdot H_2O$ and

Table 9 Crystal and refinement data for [Rh(CO)$_2${HC(pz′)$_3$}][PF$_6$], **1**$^+$[PF$_6$]$^-$, [Rh(CO)(PPh$_3$){HC(pz′)$_3$}][PF$_6$]·2CH$_2$Cl$_2$, **2**$^+$[PF$_6$]$^-$·2CH$_2$Cl$_2$, [Rh(CO)(η^2-PhC≡CPh){HC(pz′)$_3$}][PF$_6$]·1.5thf, **5**$^+$[PF$_6$]$^-$·1.5thf, [Rh{η^4-C$_4$Me$_4$C(O)}{HC(pz′)$_3$}][PF$_6$], **6**$^+$[PF$_6$]$^-$, [Rh{η^4-C$_4$Me$_2$Et$_2$C(O)}{HC(pz′)$_3$}][PF$_6$]·H$_2$O, **7**$^+$[PF$_6$]$^-$ ·H$_2$O, [Rh(CO)(η^1:η$^{1\prime}$-CHCPhCHCPh){HC(pz′)$_3$}][PF$_6$]·2CH$_2$Cl$_2$, **8**$^+$[PF$_6$]$^-$·2CH$_2$Cl$_2$ and [Rh{η^4-C$_6$H$_6$C(O)}{HC(pz′)$_3$}][PF$_6$], **10**$^+$[PF$_6$]$^-$

Compound	**1**$^+$[PF$_6$]$^-$	**2**$^+$[PF$_6$]$^-$·2CH$_2$Cl$_2$	**5**$^+$[PF$_6$]$^-$·1.5thf	**6**$^+$[PF$_6$]$^-$	**7**$^+$[PF$_6$]$^-$·H$_2$O	**8**$^+$[PF$_6$]$^-$·2CH$_2$Cl$_2$	**10**$^+$[PF$_6$]$^-$
Formula	$C_{18}H_{22}F_6N_6O_2PRh$	$C_{37}H_{41}Cl_4F_6N_6OP_2Rh$	$C_{37}H_{44}F_6N_6O_{2.50}PRh$	$C_{25}H_{34}F_6N_6OPRh$	$C_{27}H_{40}F_6N_6O_2PRh$	$C_{35}H_{38}Cl_4F_6N_6OPRh$	$C_{23}H_{28}F_6N_6OPRh$
M	602.30	1006.41	860.67	682.46	726.51	948.39	652.39
Crystal system	Monoclinic	Monoclinic	Monoclinic	Monoclinic	Monoclinic	Monoclinic	Orthorhombic
Space group (no.)	*P*2$_1$/*c*(14)	*P*2$_1$/*c*(14)	*P*2/*n*(13)	*P*2$_1$/*c*(14)	P*c*(7)	*P*2$_1$/*c*(14)	P*bca*(61)
a/Å	14.425(2)	14.565(3)	18.231(6)	8.806(4)	8.960(2)	18.592(1)	18.899(4)
b/Å	11.554(1)	16.151(3)	10.710(3)	13.867(5)	12.110(3)	12.797(1)	11.025(2)
c/Å	28.177(2)	38.248(1)	19.500(5)	22.785(6)	14.639(4)	16.722(1)	24.751(5)
α/°	90	90	90	90	90	90	90
β/°	97.19(1)	99.187(12)	93.40(3)	94.95(2)	101.89(2)	91.78(1)	90
γ/°	90	90	90	90	90	90	90
Z	8	8	4	4	2	4	8
μ/mm^{-1}	0.878	0.759	0.564	0.746	0.672	0.804	0.798
Reflections collected	29260	45331	20281	14408	10053	20233	26359
Independent reflections (R_{int})	10635	15606	6705	4887	4700	6971	4538
Final R_1,wR_2 [$I > 2\sigma(I)$]	0.0304, 0.0725	0.0673, 0.1550	0.0750, 0.1673	0.0445, 0.1039	0.0427, 0.0776	0.0490, 0.1044	0.0721, 0.1705

8$^+$[PF$_6$]$^-$·2CH$_2$Cl$_2$, slow diffusion of a concentrated CH$_2$Cl$_2$ solution of the complex into *n*-hexane at −10 °C; **5**$^+$[PF$_6$]$^-$·1.5thf, slow diffusion of a thf solution of the complex into *n*-hexane at room temperature; **6**$^+$[PF$_6$]$^-$, slow diffusion of a CH$_2$Cl$_2$ solution of the complex into diethyl ether at −10 °C; **10**$^+$[PF$_6$]$^-$, slow diffusion of a concentrated thf solution of complex **9**$^+$[PF$_6$]$^-$ into *n*-hexane at −10 °C. X-Ray diffraction measurements were made at 173 K (for **1**$^+$[PF$_6$]$^-$ and **5**$^+$[PF$_6$]$^-$–**8**$^+$[PF$_6$]$^-$) or 293 K (for **2**$^+$[PF$_6$]$^-$ and **10**$^+$[PF$_6$]$^-$). Many of the other details of the structure analyses are presented in Table 9.

The unit cells of **1**$^+$[PF$_6$]$^-$ and **5**$^+$[PF$_6$]$^-$·1.5thf each contain one disordered [PF$_6$]$^-$ anion, which has been modelled in each case with a central phosphorus atom with 100% occupancy. The major component of the disordered structure is modelled as an octahedral array of fluorine atoms about this phosphorus atom, with any remaining electron density peaks assigned as fluorine atoms in the minor orientation of the anion. The combined occupancy of the two parts was constrained to 100%. The structure of **2**$^+$[PF$_6$]$^-$·2CH$_2$Cl$_2$ contains two CH$_2$Cl$_2$ solvent molecules, one of which is disordered over two sites in an approximate 4 : 1 ratio; again the total occupancy is constrained to 100%. The solution for **5**$^+$[PF$_6$]$^-$·1.5thf contains one thf molecule, and a second that is badly disordered over a special position. The latter has been modelled with 50% occupancy with no hydrogen atoms. Hydrogen atoms were not assigned to the water molecule in **7**$^+$[PF$_6$]$^-$·H$_2$O.

CCDC reference numbers 205489–205495.

See http://www.rsc.org/suppdata/dt/b3/b302440g/ for crystallographic files in CIF format.

Acknowledgements

We thank the EPSRC for Research Studentships (to D.J.H.E and O.D.H.).

Notes and references

1 M. Akita, M. Hashimoto, S. Hikichi and Y. Moro-oka, *Organometallics*, 2000, **19**, 3744.

2 N. G. Connelly, D. J. H. Emslie, O. D. Hayward, A. G. Orpen and M. J. Quayle, *J. Chem. Soc., Dalton Trans.*, 2001, 875.

3 A. F. Hill, A. J. P. White, D. J. Williams and J. D. E. T. Wilton-Ely, *Organometallics*, 1998, **17**, 3152.

4 U. E. Bucher, A. Currao, R. Nesper, H. Ruegger, L. M. Venanzi and E. Younger, *Inorg. Chem.*, 1995, **34**, 66.

5 C. Slugovc, I. Padilla-Mart'nez, S. Sirol and E. Carmona, *Coord. Chem. Rev.*, 2001, **213**, 129.

6 N. Kitajima and W. B. Tolman, *Prog. Inorg. Chem.*, 1995, **43**, 419.

7 E. Del Ministro, O. Renn, H. Ruegger, L. M. Venanzi, U. Burckhardt and V. Gramlich, *Inorg. Chim. Acta*, 1995, **240**, 631.

8 M. Moszner, S. Wolowiec, A. Trosch and H. Vahrenkamp, *J. Organomet. Chem*, 2000, **595**, 178.

9 A. A. Purwoko, S. D. Tibensky and A. J. Lees, *Inorg. Chem.*, 1996, **35**, 7049; A. A. Purwoko and A. J. Lees, *Inorg. Chem.*, 1996, **35**, 675; C. K. Ghosh and W. A. G. Graham, *J. Am. Chem. Soc.*, 1987, **109**, 4726; S. E. Bromberg, H. Yang, M. C. Asplund, T. Lian, B. K. McNamara, K. T. Kotz, J. S. Yeston, M. Wilkens, H. Frei, R. G. Bergman and C. B. Harris, *Science*, 1997, **278**, 260; J. S. Yeston, B. K. McNamara, R. G. Bergman and C. B. Moore, *Organometallics*, 2000, **19**, 3442; E. Teuma, F. Malbosc, V. Pons, C. Serra-Le Berre, J. Jaud, M. Etienne and P. Kalck, *J. Chem. Soc., Dalton Trans.*, 2001, 2225.

10 M. A. Esteruelas, L. A. Oro, M. C. Apreda, C. Foces-Foces, F. H. Cano, R. M. Claramunt, C. Lopez, J. Elguero and M. Begtrup, *J. Organomet. Chem.*, 1988, **344**, 93; P. Ballesteros, C. Lopez, C. Lopez, R. M. Claramunt, J. A. Jimenez, M. Cano, J. V. Heras, E. Pinilla and A. Monge, *Organometallics*, 1994, **13**, 289.

11 M. A. Esteruelas, L. A. Oro, R. M. Claramunt, C. Lopez, J. L. Lavandera and J. Elguero, *J. Organomet. Chem.*, 1989, **366**, 245.

12 N. G. Connelly, D. J. H. Emslie, W. E. Geiger, O. D. Hayward, E. B. Linehan, A. G. Orpen, M. J. Quayle and P. H. Rieger, *J. Chem. Soc., Dalton Trans.*, 2001, 670.

13 R. P. Hughes, in *Comprehensive Organometallic Chemistry*, ed. G. Wilkinson, F. G. A. Stone and E. W. Abel, Pergamon Press Ltd., Oxford, 1982, vol. 5, ch. 35, p. 440.

14 R. S. Dickson and H. P. Kirsch, *Aust. J. Chem.*, 1974, **27**, 61.
15 P. A. Corrigan, R. S. Dickson, G. D. Fallon, L. J. Michel and C. Mok, *Aust. J. Chem.*, 1978, **31**, 1937.
16 R. S. Dickson and L. J. Michel, *Aust. J. Chem.*, 1975, **28**, 285.
17 R. B. King and C. A. Harmon, *Inorg. Chem.*, 1976, **15**, 879.
18 S. A. Gardner, P. S. Andrews and M. D. Rausch, *Inorg. Chem.*, 1970, **12**, 2396.
19 T. Auf der Heyde, *Angew. Chem., Int. Ed. Engl.*, 1994, **33**, 823.
20 L. M. Vallarino, *Inorg. Chem.*, 1965, **4**, 161; M. J. Cleare and W. P. Griffith, *J. Chem. Soc. A*, 1970, 2788.
21 V. Chauby, C. S. Le Berre, P. Kalck, J.-C. Daran and G. Commenges, *Inorg. Chem.*, 1996, **35**, 6354.
22 F. Malbosc, P. Kalck, J.-C. Daran and M. Etienne, *J. Chem. Soc., Dalton Trans.*, 1999, 271.
23 D. J. H. Emslie, PhD Thesis, University of Bristol, 1999.
24 W.-S. Lee and H. H. Brintzinger, *J. Organomet. Chem.*, 1977, **127**, 93.
25 J. L. Templeton and B. C. Ward, *J. Am. Chem. Soc.*, 1980, **102**, 3288.
26 J. M. O'Connor, A. Closson and P. Gantzel, *J. Am. Chem. Soc.*, 2002, **124**, 2434.
27 E. Weiss and W. Hübel, *Chem. Ber.*, 1962, **95**, 1179.
28 R. P. Dodge, *J. Am. Chem. Soc.*, 1964, **86**, 5429; G. Deganello, *Transition Metal Complexes of Cyclic Polyolefins*, Academic Press, New York, 1979, p. 106 ff.
29 E. Pretsch, W. Simon, J. Seibl and K. Biemann, in *Tables of Spectral Data for Structure Determination of Organic Compounds*, ed. W. Fresenius, J. F. K. Huber, E. Pungor, G. A. Rechnitz, W. Simon and T. S. West, Springer-Verlag, Berlin and New York, 2nd edn., 1989.
30 J. A. McCleverty and G. Wilkinson, *Inorg. Synth.*, 1990, **28**, 84.
31 N. G. Connelly and W. E. Geiger, *Chem. Rev.*, 1996, **96**, 877.
32 S. Juliá, J. M. del Mazo, L. Avila and J. Elguero, *Org. Prep. Proced. Int.*, 1984, **16**, 299.
33 D. L. Jameson and R. K. Castellano, *Inorg. Synth.*, 1998, **32**, 59.